Metabolic Engineering 52 (2019) 190–214

Contents lists available at ScienceDirect

Metabolic Engineering

journal homepage: www.elsevier.com/locate/meteng

Regulatory non-coding sRNAs in bacterial metabolic pathway engineering

Abigail N. Leistra, Nicholas C. Curtis, Lydia M. Contreras*

McKetta Department of Chemical Engineering, University of Texas at Austin, 200 E. Dean Keeton Street Stop C0400, Austin, TX 78712, USA

ARTICLE INFO

Keywords:
Metabolic pathway engineering
Non-coding RNA
Small regulatory RNA
Antisense RNA
sRNA regulatory network
High-throughput RNA-seq

ABSTRACT

Non-coding RNAs (ncRNAs) are versatile and powerful controllers of gene expression that have been increasingly linked to cellular metabolism and phenotype. In bacteria, identified and characterized ncRNAs range from trans-acting, multi-target small non-coding RNAs to dynamic, cis-encoded regulatory untranslated regions and riboswitches. These native regulators have inspired the design and construction of many synthetic RNA devices. In this work, we review the design, characterization, and impact of ncRNAs in engineering both native and exogenous metabolic pathways in bacteria. We also consider the opportunities afforded by recent high-throughput approaches for characterizing sRNA regulators and their corresponding networks to showcase their potential applications and impact in engineering bacterial metabolism.

1. Introduction

The firm establishment of microbes as viable means of producing valuable compounds has led to the development of methods to expand their natural biosynthetic capabilities (Lee et al., 2012; Nielsen and Keasling, 2016). A large part of this success can be tracked to creative solutions of the metabolic engineering field, which addresses challenges in optimization of microbial nutrient flux through native and/or heterologous pathways (Stephanopoulos and Sinskey, 1993). Traditionally, metabolic pathways are optimized by rationally knocking out genes encoding enzymes in competing pathways or by introducing more copies of genes encoding key pathway enzymes to the genome (Nielsen and Keasling, 2016). Protein engineering approaches have also been applied to fine-tune single pathway steps (Marcheschi et al., 2013). Additionally, random mutagenesis and screening (Lee et al., 2012) and adaptive laboratory evolution (ALE) approaches (Dragosits and Mattanovich, 2013) have been used to identify gene candidates for deletion, overexpression or redesign. Driven by the need to minimize strain development time, multiplex engineering has also become a primary focus of the field (Kang et al., 2015; Song et al., 2015). Conceptually, approaches like multiplex automated genome engineering (MAGE) allow for parallelization of directed genetic modifications and screening, decreasing the time to finding an optimized strain (Wang et al., 2009). While these approaches have proven useful, the strains they yield often reveal little mechanistic insight (Song et al., 2015). Researchers have also looked to engineer regulators, such as RNA polymerase sigma factors in *E. coli*. Here, a native multiple-target network is leveraged to simultaneously alter expression of many genes (Alper and Stephanopoulos, 2007).

Non-coding RNAs (ncRNAs) offer an additional suite of tools for engineering metabolic pathways. Broadly, ncRNAs in bacteria are comprised of trans-acting and cis-acting RNAs (Vazquez-Anderson and Contreras, 2013; Villa et al., 2017). Trans-acting ncRNAs, most of which are referred to as small RNAs (sRNAs), are typically 50 – 400 nucleotides in length and present imperfect complementarity for their target mRNAs (Storz et al., 2011). sRNAs can bind and regulate multiple target mRNAs (Wagner and Romby, 2015), frequently via global RNA chaperones (like Hfq) (Vogel and Luisi, 2011), to modulate their transcription termination, stability, and/or translation (Gottesman and Storz, 2011; Kavita et al., 2018; Nitzan et al., 2017). Cis-acting ncRNAs, such as ligand-responsive riboswitches or sRNA-responsive toehold switches, provide dynamic control of single genes and/or operons (Mellin and Cossart, 2015). Importantly, development and application of new high-throughput techniques that probe RNA structure and function *in vivo* is expanding our understanding of ncRNAs within their native pathways to include increasingly diverse and complex mechanisms and target networks (Hör et al., 2018; Mihailovic et al., 2018).

Non-coding RNAs have been touted as highly programmable in their structure and interactions via Watson-Crick base pairing (Kushwaha et al., 2016). Based on this knowledge and on examples of native ncRNA regulators, synthetic ncRNA regulators have been frequently applied to engineer metabolic pathways. For example, user-designed antisense RNAs (asRNAs) contain anywhere from 10 to greater than 200 nucleotides of complementarity to the mRNA of an enzyme of interest. The asRNA binds the mRNA by base pairing and knocks down its activity by directly blocking translation or destabilizing the mRNA.

* Corresponding author.
E-mail address: lcontrer@che.utexas.edu (L.M. Contreras).

https://doi.org/10.1016/j.ymben.2018.11.013
Received 15 May 2018; Received in revised form 31 October 2018; Accepted 29 November 2018
Available online 01 December 2018

Typically, although not always, the target-specific antisense region is accompanied by stabilizing elements, like base-pairing 5′ and 3′ termini or an Hfq-binding scaffold borrowed from a native, well-characterized sRNA (Cho et al., 2015) (Fig. 1A I-III). Additionally, efforts have been made to design stabilizing elements *de novo* using thermodynamic modeling approaches (Rodrigo et al., 2013). These asRNA regulators have been applied in bacteria to achieve a range of target enzyme activities and impact on phenotypes (Hoynes-O'Connor and Moon, 2016; Na et al., 2013; Park et al., 2014). A main advantage of asRNA systems, especially relative to genomic deletions, is their tractability as one can easily sample the impacts of (1) multiple strain backgrounds and (2) multiple levels of target enzyme knockdown on product yields (Na et al., 2013).

In addition to synthetic asRNAs, native bacterial sRNA regulators are being co-opted as tools for pathway engineering. Given that bacterial sRNAs have been identified and characterized as native mediators of stress responses (Kavita et al., 2018; Nitzan et al., 2017), they hold promise for engineering production phenotypes, which tend to place

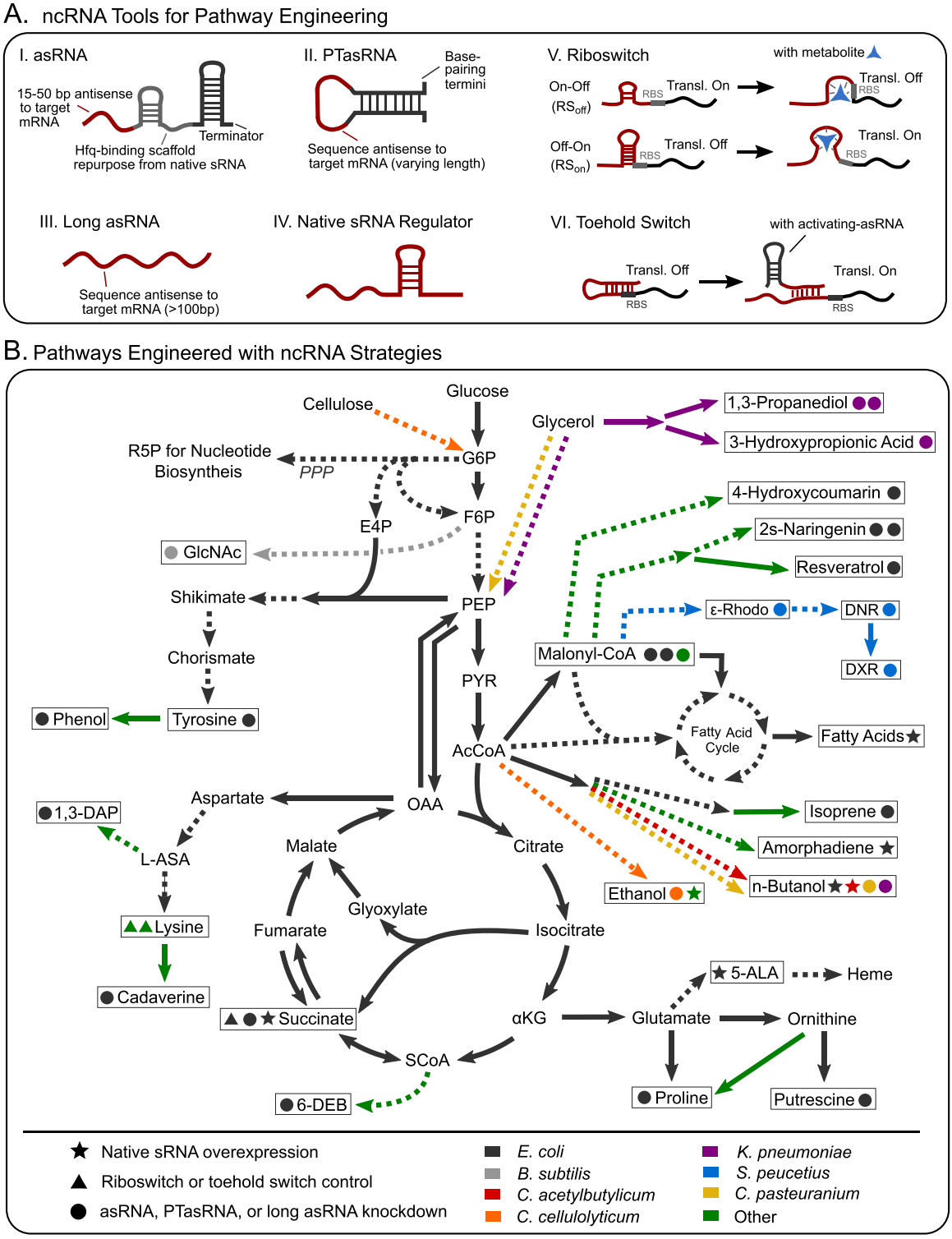

(caption on next page)

Fig. 1. Pathways engineered with ncRNA strategies. (A) ncRNA-based tools for pathway engineering. Knockdown of target mRNA expression is achieved with (I) antisense RNA (asRNA), (II) paired-termini antisense RNA (PTasRNA), and (III) long asRNA. (IV) Native sRNA regulators are used as handles to control expression of their targets. (V) Riboswitches and (VI) toe-hold switches dynamically turn on or off expression of a target mRNA in response to a ligand or activating asRNA. (B) Network of pathways engineered with ncRNA strategies. All reviewed compounds overproduced by ncRNA-based pathway engineering strategies are boxed (acid tolerance phenotype not pictured). Relevant enzymatic connections to each other, key carbon sources, glycolysis intermediates, and TCA cycle intermediates are indicated by arrows (solid, one step; dashed, multiple steps). Symbols boxed with compound names indicate the type of ncRNA engineering strategy applied to the compound's pathway (knockdown mediated by asRNA, PTasRNA or long asRNA, native sRNA overexpression, or addition of a riboswitch or toehold switch upstream of a target gene; see in-figure legend). Symbol color indicates the host organism used for compound overproduction with the indicated ncRNA pathway engineering strategy (see in-figure legend). Pathway arrows are colored to indicate the organism from which the pathways are imported (if not native). Pathways shared between *E. coli* and other organisms are colored dark gray. Red, orange, yellow, purple, light gray, blue, and green pathway arrows are unique to their corresponding organism relative to *E. coli*. Abbreviations are as follows: G6P, glucose-6-phosphate; F6P, fructose-6-phosphate; E4P, erythrose-4-phosphate; R5P, ribulose-5-phophate; PPP, pentose phosphate pathway; PEP, phosphoenol pyruvate; PYR, pyruvate; Ac-CoA, acetyl-Coenzyme A (CoA); OAA, oxaloacetate; aKG, alpha-ketoglutarate; S-CoA, succinyl-CoA; L-ASA, L-aspartate 4-semialdehyde; 1,3-DAP, 1,3-diaminopropane; GlcNAc, N-acetylglucosamine; 5-ALA, 5-aminolevuinic acid; ε-rhodo, ε-rhodomycinone; DNR, duanorubicin; and DXR, doxorubicin.

bacteria under stress (Nielsen and Keasling, 2016). For example, overexpression of native sRNA regulators improves titers of amino acids, fatty acids, 5-amino-levulinic acid and heterologous butanol (Jones et al., 2016; Kang et al., 2012; Li et al., 2014; McKee et al., 2012). One advantage of native sRNA regulators is that they frequently regulate many targets, such that overexpressing the regulator simultaneously controls the expression of many genes. Compared to transcription factors that require protein synthesis, using multi-target sRNA regulators in pathway engineering imparts relatively low metabolic loads (Altuvia and Wagner, 2000; Kang et al., 2014).

The history of ncRNAs in strain engineering has been well-reviewed (Chaudhary et al., 2015a; Kang et al., 2014) as well as the advantages of asRNA-mediated knockdown relative to genome engineering approaches (Song et al., 2015). Additionally, works have reviewed available ncRNA tools (Jang et al., 2018; Qi and Arkin, 2014; Vazquez-Anderson and Contreras, 2013), multiple approaches for constructing synthetic asRNAs (Cho et al., 2015), and rules for designing the antisense region in particular (Lee and Moon, 2018). In this review, we consider examples of ncRNAs applied for metabolic engineering from a pathway perspective (Fig. 1B). We document the (i) rationale of ncRNA regulator design and target selection, (ii) mechanism of pathway impact, (iii) engineering outcome (yield/titer), and (iv) subsequent conclusions drawn about bacterial metabolism from ncRNA incorporation. In this way, particular attention is paid to the application and impact of asRNAs (Fig. 1A I-III) and native sRNA regulators (Fig. 1A IV), rather than riboswitches and toehold switches (Fig. 1A V-VI), as the former have been most frequently used to engineer metabolic pathways. Specifically, we discuss the contribution of ncRNAs in engineering the following pathways and products: (i) amino acid and tricarboxylic acid cycle-derived products, (ii) products with flux through malonyl-CoA and acetyl-CoA, (iii) alcohol biosynthesis and tolerance, (iv) acid resistance and tolerance phenotypes, (v) diols and related acids, (vi) doxorubicin biosynthesis, and (vii) n-acetylglucosamine biosynthesis (Fig. 1B).

Several themes emerge from the studies reviewed and we discuss the guidance they offer future ncRNA-based pathway engineering. Table 1 summarizes the ncRNA strategies used to engineer each pathway discussed and the broader themes they demonstrate. These include (i) the importance of tuning asRNA knockdown level for pathway optimization; (ii) the role that flux analysis, omics data or a prior notable observation can play in selecting impactful enzymatic nodes to target; and (iii) the utility of targeting or overexpressing regulators to simultaneously impact expression of multiple genes. Additionally, we discuss how (iv) the interdependency of pathway modifications and (v) the variations of growth conditions between studies can hinder generalization of results. Importantly, we emphasize the ability of native sRNAs to support complex phenotypes, as the use of native sRNAs is now more accessible with recent advances in high-throughput sRNA characterization techniques.

2. Design and application of ncRNAs to engineer metabolic pathways

2.1. Biosynthesis of amino acid and TCA cycle-derived compounds

One group of pathways that has received considerable engineering interest is central carbon metabolism and amino acid metabolism. Several tricarboxylic acid (TCA) cycle intermediates, amino acids, and their closely-related derivative compounds have been engineered for overproduction in *E. coli* and in other bacteria with ncRNA strategies (Table 1). In most of these instances, asRNAs are used to knockdown expression of enzymes that compete with the desired pathways for key intermediate compounds, while a few instances utilize dynamic ncRNA control schemes or native sRNA regulators. Additionally, ncRNA control strategies are frequently applied in tandem with previously-demonstrated, genome-level modifications. Thus, incremental pathway engineering progress for an array of compounds is attributed to ncRNAs relative to controls that lack only the ncRNA strategy. Quantifying the impact of the ncRNA strategy with respect to the prior best producing strain, rather than a wild type strain, potentially limits the observed impact of the ncRNA strategy. However, applying ncRNA strategies in the context of other genome modifications clearly illustrates the flexibility asRNAs provide for testing multiple (i) genetic strain backgrounds and (ii) target enzyme knockdown levels to optimize pathway titer.

The following examples demonstrate the utility of targeting native regulators or overexpressing native sRNA regulators to impact expression of multiple genes. They also showcase how flux analysis and/or omics data can be used to inform selection of genes for knockdown. Closely related products are reviewed together to highlight future applications of ncRNA strategies in engineering overproduction of other compounds in the pathway.

2.1.1. Tyrosine and phenol

Tyrosine is an aromatic amino acid naturally synthesized from phosphoenol pyruvate (PEP) and erythrose-4-phosphate (E4P, a 4-carbon compound of the pentose-phosphate pathway) via shikimate and chorismate intermediates in *E. coli* (Lütke-Eversloh et al., 2007) (Fig. 1B), (Table 2). Efforts to engineer scalable tyrosine biosynthesis schemes have predominantly focused on *E. coli* and *Corynebacterium glutamicum* (Ikeda, 2005). Progress made in engineering the tyrosine pathway through traditional, non-ncRNA approaches has been thoroughly reviewed (Rodriguez et al., 2014). These strategies include relieving native pathway regulation and identifying and optimizing bottleneck enzymatic steps (Ikeda, 2005; Juminaga et al., 2012; Lütke-Eversloh and Stephanopoulos, 2007, 2008).

Building upon these approaches, asRNA-mediated knockdown of several genes was attempted to improve tyrosine titer (Na et al., 2013). The authors selected 4 target genes to knock down: *tyrR* mRNA, a transcription factor that represses multiple genes in the tyrosine pathway (Pittard et al., 2005); *csrA* mRNA, a post-transcriptional

Table 1
Pathways and products engineered with ncRNA strategies.

Product/Phenotype	Organism	Observed Themes[a]	ncRNA Engineering Strategy	ncRNA mRNA Target(s)	Yield/Titer in Flask Culture (% improvement to no RNA control[b])	Other Genetic Modification?	Reference
Tyrosine	*E. coli*	R, T	asRNA (as + hfq scaffold)	KD *csrA* and KD *tyrR*	2 g/L (approximately 100% increase)	yes	(Na et al., 2013)
Phenol	*E. coli*	R	asRNA (as + hfq scaffold)	KD *csrA* and KD *tyrR*	419 mg/L	yes	(Kim et al., 2014)
Cadaverine	*E. coli*	ID	asRNA (as + hfq scaffold)	KD *murE*	2.15 g/L (31% increase in high cell density fed batch culture)	yes	(Na et al., 2013)
Lysine	*Corynebacterium glutamicum*	DC	Riboswitch (RSoff, genomic)	*gltA*	0.227 mol lysine/mol glucose (63% increase)	yes	(Zhou and Zeng, 2015b)
Lysine	*Corynebacterium glutamicum*	DC	Riboswitch (RSon, genomic)	*lysE*	0.267 mol lysine/mol glucose (20% increase)	yes	(Zhou and Zeng, 2015a)
1,3-Diaminopropane	*E. coli*	T	asRNA (as + hfq scaffold)	KD *pykF*	Approximately 381 mg/L (35% increase)	yes	(Chae et al., 2015)
Putrescine	*E. coli*	T, E, FA	asRNA (as + hfq scaffold)	KD *argF* and KD *glnA*	KD argF only: 2.7 g/L (61% inc); KD glnA only: 2.1 g/L (25% inc); KD argF and glnA: 43 g/L in high density fed batch culture (78% inc)	yes	(Noh et al., 2017)
L-Proline	*E. coli*	T	asRNA (as + hfq scaffold)	KD *glnA* and KD *argF*	2.02 g/L (7-fold increase)	yes	(Noh et al., 2017)
5-Aminolevulinic Acid	*E. coli*	R	Overexpress RyhB sRNA	*sdhDCAB*, *acnAB*, *fumA*, *cydAB*, *hemB**, *hemH** (repressed)	1.78 g/L (16% increase)	yes	(Li et al., 2014)
Succinate (anaerobic growth)	*E. coli*		asRNA (as + hfq scaffold)	KD *pykF*	30.12 mM (3.6 g/L) succinate (20% inc); 13.22 mM acetate (45% dec)	yes	(Zhao et al., 2016)
Succinate	*E. coli*	R, SCP	Overexpress RyhB sRNA	*sdhDCAB*, *acnAB*, *fumA* (repressed)	2.2 g/L succinate (5-fold inc); 1.8 g/L acetate (3-fold inc)	yes	(Kang et al., 2012)
Succinate (anaerobic growth)	*E. coli*	DC	Synthetic toe-hold switch (genomic) and asRNA (as + hfq scaffold)	THS *ecaA* and *pepC*; KD *mgtC*	31.2 g/L succinate (13% increase)	yes	(Wang et al., 2018a)
6-Deoxyerythronolide B (20 mM propionate added)	*E. coli*	FA, O	asRNA (as + hfq scaffold)	KD *guaB* and KD *zwf*	210.4 mg/mL (4-fold increase) (120 h)	yes	(Meng et al., 2015)
Malonyl-CoA	*E. coli*	E, GC	PTasRNA	KD *fabD*	0.25 nmol/ mg DCW (4.5 fold-increase) (12 h)	no	(Yang et al., 2015)
Malonyl-CoA	*E. coli*	E, IC, T, GC	PTasRNA	KD *fabB* and KD *fabF*	0.88 nmol/mg DCW (8.8-fold increase) (48 h)	no	(Wu et al., 2014)
Malonyl-CoA	*Synechocystis* sp. *PCC 6803*	E	asRNA (as + hfq scaffold + hfq; genomic)	KD *fabF*, KD *fabH*, and KD *fabD*	0.07 μg/L (41% increase) (48 h)	yes	(Sun et al., 2018)
4-Hydroxycoumarin (polyketide)	*E. coli*	E	PTasRNA	KD *fabD*	271 mg/L 4-hydroxycoumarin (2.5-fold increase) (24 h)	yes	(Yang et al., 2015)
Resveratrol (polyketide; 1 mM p-coumaric acid added)	*E. coli*	E	PTasRNA	KD *fabD*	268.2 mg/L (70% increase) (24 h)	yes	(Yang et al., 2015)
(2S)-Naringenin (polyketide; 1 mM p-coumaric acid added)	*E. coli*	E, GC	PTasRNA	KD *fabD*	91.3 mg/L (50% increase) (24 h)	yes	(Yang et al., 2015)
(2S)-Naringenin (polyketide; 3 mM tyrosine and 2 g/L malonate added)	*E. coli*	E, IC, T, GC	PTasRNA	KD *fabB* and KD *fabF*	391 mg/L (4.3-fold increase) (48 h)	yes	(Wu et al., 2014)
Natural Fatty Acids	*E. coli*	R, O, SCP	Overexpress CsrB sRNA	Sequester CsrA; Indirectly impact CsrA targets	430 mg/L (85% increase) (48 h)	yes	(McKee et al., 2012)
Amorphadiene	*E. coli*	R, O, SCP	Overexpress CsrB sRNA	Sequester CsrA; Indirectly impact CsrA targets	93 mg/L (55% increase) (48 h)	yes	(McKee et al., 2012)
Isoprene	*E. coli*		long asRNA	KD *ispA*, KD *ispU*, and KD *ispB*	16 mg/L (8-fold increase) (approximately 24 h)	yes	(Liu et al., 2015)
n-Butanol (pathway induced with arabinose)	*E. coli*	R, O, SCP	Overexpress CsrB sRNA	Sequester CsrA; Indirectly impact CsrA targets	90 mg/L (88% increase) (48 h)	yes	(McKee et al., 2012)

(*continued on next page*)

Table 1 (*continued*)

Product/Phenotype	Organism	Observed Themes[a]	ncRNA Engineering Strategy	ncRNA mRNA Target(s)	Yield/Titer in Flask Culture (% improvement to no RNA control[b])	Other Genetic Modification?	Reference
Butanol (anaerobic growth)	*Clostridium acetobutylicum*	R, IC, SCP	Overexpress 6 S sRNA	Sequester sigma 70 to inactivate housekeeping gene transcription	180 mM butanol (13.3 g/L) (20% increase) (72 h)	no	(Jones et al., 2016)
Butanol (anaerobic growth, 50 g/L glycerol feed)	*Clostridium pasteurianum*	IC	long asRNA	KD *hydA*	10 g/L butanol (12% increase) (40–50 h)	no	(Pyne et al., 2015)
1-Butanol (20 g/L glycerol and 5 g/L glucose feed)	*Klebsiella pneumoniae*		long asRNA	KD *gdrf1* and *2*, KD *dhaB1*, *2*, and *3*	20.5 mg/L butanol (37% inc); 1.1 g/L 1,3-PDO (71% dec) (24 h)	yes	(Wang et al., 2014)
Ethanol/limit Acetate (anaerobic growth, 10 g/L cellulose feed)	*Clostridium cellulolyticum*	E, T	long asRNA	KD *pta*	1.96 g/L ethanol (86% inc); 0.5 g/L acetate (33% dec); 2 ± 8 mg/L lactate (97% dec)	yes	(Xu et al., 2017)
Acid Tolerance	*E. coli*	R, SCP	Overexpress ArcZ, RprA, DsrA sRNAs	*rpoS* mRNA	8500-fold greater survival in acidic media (1 h exposure)	no	(Gaida et al., 2013)
Acid Tolerance	*E. coli*	R, SCP	Overexpress DsrA sRNA	*rpoS* mRNA	106-fold greater survival in acidic media (1 h exposure)	no	(Gaida et al., 2013)
Acid Tolerance	*E. coli*	R, SCP	Overexpress RprA sRNA	*rpoS* mRNA	3-fold greater survival in acidic media (1 h exposure)	no	(Gaida et al., 2013)
Acid Tolerance	*E. coli*	R, SCP	Overexpress ArcZ sRNA	*rpoS* mRNA	5-fold greater survival in acidic media (1 h exposure)	no	(Gaida et al., 2013)
1,3-Propanediol	*Klebsiella pneumoniae*	IC	PTasRNA	KD *budA*	21.5 g/L 1,3-PDO (10% inc), 3 g/L 2,3-BDO (40% dec) (36 h)	no	(Lu et al., 2016a)
1,3-Propanediol	*Klebsiella pneumoniae*	IC	PTasRNA	KD *budB*	21.5 g/L 1,3-PDO (10% inc), 3 g/L 2,3-BDO (40% dec) (36 h)	no	(Lu et al., 2016a)
3-Hydroxyproprionic acid	*Klebsiella pneumoniae*	T	long asRNA	KD *ldh*(1–4) and KD *poxB*	1.29 g/L 1,3-HP (70% inc); 1.46 g/L lactic acid (24% dec); 0.6 g/L acetic acid (50% dec) (24 h)	yes	(Li et al., 2016a)
Doxorubicin	*Streptomyces peucetius*	R, GC	PTasRNA	KD *doxR*	5.8-fold increase doxorubicin (84 h)	no	(Chaudhary et al., 2015b)
Duanorubicin	*Streptomyces peucetius*	R, GC	PTasRNA	KD *doxR*	3.6-fold increase duanorubicin (84 h)	no	(Chaudhary et al., 2015b)
ε-Rhodomycinone	*Streptomyces peucetius*	R, GC	PTasRNA	KD *doxR*	1.4-fold increase ε-rhodomycinone (84 h)	no	(Chaudhary et al., 2015b)
N-Acetylglucosamine	*Bacillus subtilis*	T	asRNA (as + hfq scaffold + hfq)	KD *pfk* and KD *glmM*	8.3 g/L (2.3-fold increase) (30 h) (31.7 g/L high cell density fermentation (46 h))	yes	(Liu et al., 2014b)

[a] Legend for Observed Themes: R, Targeting or overexpressing **r**egulators affects multiple genes; SCP, native **s**RNA regulators **s**upport **c**omplex **p**henotypes; T, **t**uning knockdown level allows optimization; E, asRNAs allow **e**ssential genes or gene pairs to be targeted; GC, impacts of ncRNA strategy shown to vary over **g**rowth **c**onditions; DC, **d**ynamic **c**ontrol is achieved by ncRNA strategy; ID, **i**nter**d**ependency of pathway modifications; FA, **F**lux **a**nalysis used to identify targets for knockdown; IC, **i**nformed **c**hoice of target knockdown based notable on prior observations.

[b] Percent improvement compared a no ncRNA control, i.e. the effect of the ncRNA regulator described in the "ncRNA Engineering Strategy" and "ncRNA Target(s)" columns. Increase abbreviated to "inc" and decrease abbreviated to "dec" for spacing if necessary.

Table 2
Alternative production methods of reviewed compounds.

Product/Phenotype	Alternative approaches for manufacture
Tyrosine	(1) Isolation from biological products including casein and corn or wheat gluten. (2) Fermentation of engineered microorganism. (Bruno, 1956; Cardinal, 1953; Lütke-Eversloh et al., 2007; Maurice, 1939).
Phenol[a]	(1) Oxidation of cumene followed by acid-mediated cleavage produces phenol and acetone (Schmidt, 2005). (2) Hydroalkylation of benzene, oxidation, and acid-mediated cleavage yields phenol and cyclohexanone (Dakka et al., 2012).
Cadaverine	Fermentation of high lysine-producing organism with lysine decarboxylase activity (Kazami and Mimizuka, 2014).
Lysine[b]	Fermentation of engineered *Corynebacterium glutamicum* (Kreutzer et al., 2001; Leuchtenberger et al., 2005; Nielsen and Keasling, 2016).
1,3-Diaminopropane	(1) Amination of acrylonitrile with ammonia, followed by catalytic reduction in alcohol solvent (Ohinata and Takayanagi, 2003). (2) Fermentation of engineered microorganism (Chae et al., 2015).
Putrescine	(1) Fermentation of engineered microorganism with increased ornithine decarboxylase activity (Eppelmann et al., 2013). (2) Reaction of hydrogen cyanide and acrylonitrile to succinonitrile, followed by hydrogenation (Sanders et al., 2007).
L-Proline	(1) Fermentation of engineered *Corynebacterium glutamicum*. (2) Isolation from hydrolyzed protein. (Leuchtenberger et al., 2005; Yoshinaga et al., 1974).
5-Aminolevulinic Acid	(1) Fermentation of engineered *E. coli* or *C. glutamicum* (Lin et al., 2009; Liu et al., 2014a; Yang et al., 2016a). (2) Photo-oxidation of N-protected furfurylamine, followed by hydrogenation and acid hydrolysis (Sasaki et al., 2002; Takeya et al., 1996). (3) Bromination of levulinic acid in methanol, followed by addition of diformylamide and acid hydrolysis (Bozell et al., 2000).
Succinate[c]	(1) Petrochemically-derived butane is converted to maleic anhydride, which is catalytically hydrogenated to succinate (Benjamin et al., 2014; Zeikus et al., 1999). (2) Fermentation of engineered microorganisms (McKinlay et al., 2007).
6-Deoxyerythronolide B (polyketide; macrocyclic core of erythromycin)	Biosynthesis in *Saccharopolyspora erythraea* or *Streptomyces* species (Katz et al., 1998; Pfeifer et al., 2001).
Malonyl-CoA	Mainly targeted as an intermediate to support polyketide biosyntheses in engineered microorganisms (Sun et al., 2018; Wu et al., 2014; Yang et al., 2015).
4-Hydroxycoumarin (polyketide)	(1) Syntheses from petrochemicals, such as reaction of phenol with Meldrum's acid, followed by treatment with Eaton's reagent and hydration for cyclization (Gao et al., 2010). (2) Fermentation of engineered *E. coli*. (Lin et al., 2013).
Reseveratrol (polyketide)	(1) Isolated from plants, like *Polygonum cuspidatum* and *Festuca versuta* (Nonomura et al., 1963; Powell et al., 1994). (2) Fermentation of engineered *E. coli* (Lim et al., 2011).
(2 S)-Naringenin (polyketide)	(1) Extraction from citrus fruits (Gaffield et al., 1975). (2) Fermentation of engineered *E. coli* (Hwang et al., 2003).
Amorphadiene (isprenoid; immediate artemisinin precursor)	(1) Extraction from leaves of *Artemisia annua* herb. (2) Fermentation of engineered *E. coli* or *S. cerevisiae*.(Hale et al., 2007; Martin et al., 2003; Ro et al., 2006).
Isoprene[d]	(1) Byproduct of ethylene production, via thermal cracking of oil hydrocarbons (Lybarger, 2014; Sundaram et al., 2010; Vickers and Sabri, 2015). (2) Fermentation of engineered microorganism (Cervin et al., 2016).
n-Butanol[e]	(1) The Oxo reaction of propylene, obtained from steam or catalytic cracking of oil hydrocarbons, yields n-butyraldehyde, which is catalytically hydrogenated to produce n-butanol (Billig, 2001, 2003; Calamur and Carrera, 2005). (2) Fermentation of engineered microorganisms, particularly *C. acetobutylicum* (Lütke-Eversloh and Bahl, 2011).
Ethanol[f]	(1) Fermentation of pre-processed corn by *S. cerevisiae* or other engineered microorganisms. (2) Catalytic hydration of ethylene. (Logsdon, 2004).
1,3-Propanediol[g]	(1) Hydration of acrolein to 3-hydroxypropionaldehyde, followed by hydrogenation to 1,3-propanediol. (2) Hydroformylation of ethylene oxide to 3-hydroxypropionaldehyde, followed by hydrogenation to 1,3-propanediol. (3) Fermentation of engineered *E. coli* or other microorganisms. (Sun et al., 2014).
3-hydroxypropionic acid	Fermentation of engineered microorganisms (Kumar et al., 2014).
Doxorubicin	Fermentation of *Streptomyces peucetius* (Malla et al., 2010b).
Duanorubicin	Fermentation of *Streptomyces peucetius* (Malla et al., 2010b).
ε-Rhodomycinone	Fermentation of *Streptomyces peucetius* (Malla et al., 2010b).
N-Acetylglucosamine	(1) Acid hydrolysis of chitin extracted from shellfish shells. (2) Fermentation of engineered microorganisms. (Chen et al., 2010; Liu et al., 2014b)

[a] Estimated $17 billion market by 2022 (Persistence Market Research, 2017).
[b] Part of estimated $6.82 billion food amino acid market by 2022 (Markets and Markets, 2017).
[c] Estimated $993 million bio-succinic acid market by 2020 (Grand View Research, 2014).
[d] Estimated $1.17 billion market in 2016 (Grand View Research, 2017b).
[e] Estimated $4.18 billion market in 2017 and projected $5.58 Billion market by 2022 (Markets and Markets, 2018).
[f] Estimated $64.5 Billion market in 2016 and projected $115.7 Billion market by 2025 (Grand View Research, 2017a).
[g] $310.5 Million market in 2014 and projected $621.2 million market by 2021 (Markets and Markets, 2015).

regulator that impacts expression of glycolysis (Esquerré et al., 2016; Morin et al., 2016) and TCA cycle enzymes (Sowa et al., 2017); *ppc* mRNA, which catalyzes competing consumption of PEP to oxaloacetate (OAA); and *pgi* mRNA, which interconverts glucose-6-phosphate (G6P) and fructose-6-phosphate (F6P). The asRNAs each contained a 24 nucleotide RNA sequence antisense to the start codon region of their mRNA target, a structured hfq-binding sequence repurposed from the MicC *E. coli* sRNA, and a synthetic terminator hairpin (as shown in Fig. 1A I). The asRNA regulators were overexpressed on a plasmid with several genes previously used in tyrosine pathway engineering: *ppsA*, *tktA*, *aroG**, *aroF*, *aroK*, *tyrA**, and *tyrC*, a gene native to *Zymomonas mobilis* which converts prephante to tyrosine directly, rather than in two steps via *tyrA* and *tyrB* (Lütke-Eversloh and Stephanopoulos, 2008) (Fig. 2A). The asterisks on *aroG** and *tyrA** genes indicate single amino acid mutants of *aroG* and *tyrA* that remove feedback inhibition by their enzymatic end products (Lütke-Eversloh and Stephanopoulos, 2007).

Simultaneous knockdown of the *tyrR* and *csrA* mRNAs in the S17-1 *E. coli* strain (K-12 derivative) achieved the greatest production of tyrosine: 2 g/L in flask culture (approximately 100% increase relative to a no asRNA control) and 21.9 g/L in high-density fed-batch conditions (Table 1) (Na et al., 2013). Importantly, varying the interaction energy of the anti-*csrA* sRNA (i.e., the asRNA targeting *csrA*) and the *csrA* mRNA in the S17-1 strain provided for a 2-fold range of tyrosine titer (1–2 g/L). While the highest titer is clearly desired in this instance, the

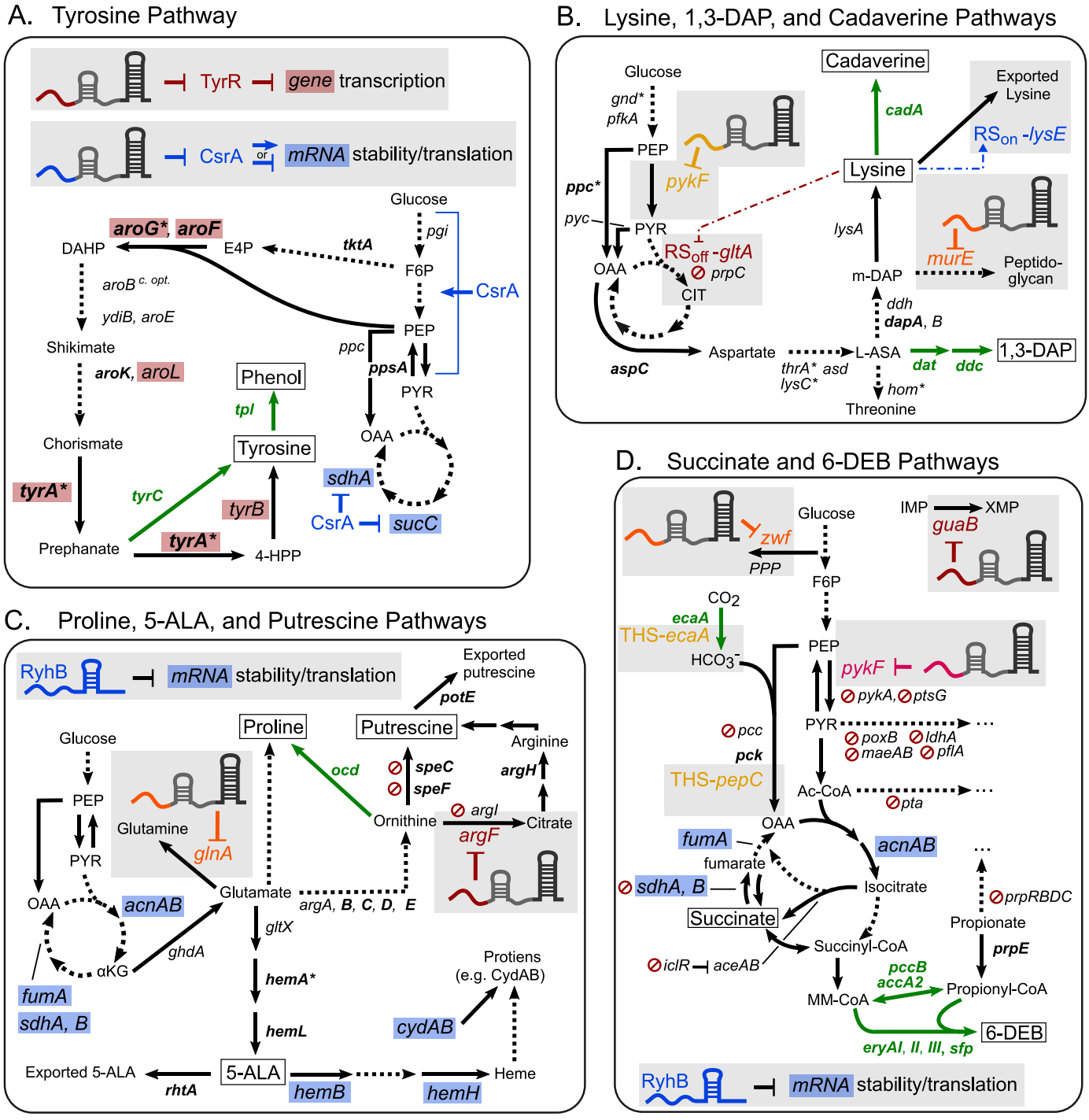

Fig. 2. ncRNA-driven production of amino acids, TCA cycle intermediates, and derived products. Pathway diagrams include solid arrows to indicate single enzymatic steps and dashed arrows to indicate multiple enzymatic steps. Boxed, large type compounds are overproduced by an ncRNA-based pathway engineering strategy. asRNA, PTasRNA, long asRNA and native sRNA icons from Fig. 1A are used to indicate the type of ncRNA tool and target(s). Other pathway engineering strategies used with the ncRNA-based strategy are depicted: gene overexpression (**bold type**), exogenous gene overexpression (**green bold type**), enzyme de-regulation mutations (*), and gene deletion (red circle-line "not" symbol). (A) Tyrosine pathway. Tyrosine and phenol overproduction is achieved in *E. coli* by asRNA-mediated knockdown of the TyrR and CsrA regulator proteins. Genes shaded red are transcriptionally controlled by TyrR; genes shaded blue are regulated at the mRNA level by CsrA. Activation of glycolysis enzymes by CsrA is shown by a blue arrow and bracket (direct interactions not fully confirmed). (B) Lysine, cadaverine, and 1,3-diaminoproane (1,3-DAP) pathways. Overproduction is driven in *E. coli* or *C. glutamicum* by knockdown of peptidoglycan biosynthesis with anti-*murE*, knockdown of glycolysis with anti-*pykF*, and lysine-responsive control of *lysE* and *gltA* with riboswitches (denoted as RS_{on}-*lysE* and RS_{off}-*gltA*). (C) Proline, 5-ALA, and Putrescine pathways. Overproduction is engineered in *E. coli* with anti-*glnA* and anti-*argF* sRNAs to knock down competing reactions of glutamate and ornithine, respectively, and overexpression of the RyhB native sRNA regulator. Genes that are repressed at the mRNA level by RyhB are shaded blue (direct targets, except *hemB* and *hemH* are likely targets). (D) Succinate and 6-deoxyerythronucleotide B (6-DEB) pathways. Product enrichment is achieved by anti-*zwf*, anti-*guaB*, and anti-*pykF* sRNAs, toehold switch control of *ecaA* and *pepC* (denoted as THS-*ecaC*, THS-*pepC*), and RyhB overexpression. Genes that are repressed at the mRNA level by RyhB are shaded blue. Ellipses indicate consumption of intermediates into other pathways. Abbreviations are as follows: F6P, fructose-6-phosphate; PEP, phosphoenol pyruvate; PYR, pyruvate; Ac-CoA, acetyl-CoA; OAA, oxaloacetate; E4P, erythrose-4-phosphate; DAHP, 3-deoxy-D-arabino-heptulosonate; 4-HPP, 4-hydroxyphenyl-pyruvate; CIT, citrate; L-ASA, L-aspartate 4-semialdehyde; m-DAP, meso-2,6-diaminopimelate; 5-ALA, 5-aminolevulinic acid; IMP, inosine monophosphate; XMP, xanthosine monophosphate; MM-CoA, methylmalonyl-CoA; and 6-DEB, 6-deoxyerythronucleotide B.

ability to easily access a range of tyrosine production with a small library of asRNAs may prove useful in engineering other tyrosine-dependent phenotypes.

Remarkably, the best result achieved with asRNA knockdown approximately matches a 2.2 g/L tyrosine titer achieved in an earlier study that fine-tuned overexpression of all pathway enzymes based on proteomics and metabolomics (Juminaga et al., 2012). This comparison highlights the impact of targeting an organism's native regulators in pathway engineering. The TyrR transcription factor represses transcription of *aroG* (Baseggio et al., 1990), *aroF-tyrA* (Cobbett, 1988), *aroL* (Heatwole and Somerville, 1992; Lawley and Pittard, 1994), and *tyrB* (Gama-Castro et al., 2016; Yang et al., 2002) in an aromatic amino-acid dependent manner. Thus, knocking down the *tyrR* mRNA likely offers coordinated upregulation of multiple steps of the aromatic amino acid biosynthesis pathways. Additionally, results demonstrate how affecting a more distant regulator, CsrA, could favorably impact fluxes through central carbon metabolism (glycolysis and TCA cycle) to improve specific pathway titer. asRNA-mediated knockdown makes screening for these useful targets easier. Given the wide scope of targets and cellular effects of the TyrR and CsrA regulators, the anti-*tyrR* anti-*csrA* sRNAs may prove useful for improving production of tryptophan and/or phenylalanine as well (McKee et al., 2012; Yakandawala et al., 2008).

Plasmid-based asRNA knockdown additionally enables easy screening in multiple strain backgrounds. For instance, expressing the anti-*tyrR* and anti-*csrA* sRNAs in multiple different *E. coli* strains resulted in tyrosine titers ranging from 0.2 to 2 g/L (Na et al., 2013). A similar approach was used to optimize biosynthesis of phenol. Although phenol is not natively produced in *E. coli*, heterologous expression of tyrosine phenol lysine (*tpl*) from *Pasteurella multocida* (Wierckx et al., 2005) can extend the tyrosine pathway to produce phenol (Fig. 2A). Kim and colleagues thus applied the same anti-*csrA* and anti-*tyrR* sRNAs (as in (Na et al., 2013)) in the presence of overexpressed *ppsA*, *tktA*, *aroG**, *aroF*, *aroK*, *tyrA**, *tyrC,* and *tpl* (Kim et al., 2014). Unexpectedly, the *E. coli* BL21 strain provided maximum phenol titer (419 mg/L, Table 1). This strain only produced only half as much tyrosine (1 g/L) relative to the optimal S17-1 (2 g/L) strain in the earlier work (Na et al., 2013). Given that the phenol and tyrosine pathways differ only by a single step, this comparison highlights the importance of tuning an engineering strategy even for compounds of the same pathway, particularly when one may be toxic. asRNA-mediated knockdown, rather than genomic deletion, makes screening multiple strains easier, given that a plasmid system expressing the designed asRNA can be constructed once and then easily tested in multiple strains.

2.1.2. Lysine, cadaverine, and 1,3-diaminopropane

Microbial production of lysine, naturally produced from oxaloacetate via aspartate (Fig. 1B), is used at the industrial scale for feed additives (Nielsen and Keasling, 2016). The lysine bioproduction process uses engineered *Corynebacterium glutamicum*, a gram positive bacterium that has received attention for its amino acid production capabilities (Wendisch et al., 2006). Improvements in lysine pathway yields have been achieved by de-regulating enzymatic feedback inhibition of relevant enzymes (Chen et al., 2014, 2011b; Ohnishi et al., 2005, 2002; Wendisch et al., 2006) and by adding additional copies of pathways enzymes to the genome (Ooyen et al., 2012) (Fig. 2B). Dynamic control of lysine biosynthesis in *C. glutamicum* is a comparatively understudied approach. *C. glutamicum* produces most lysine in stationary growth phase, after most biomass has already been generated (Chen et al., 2014). As such, lysine-responsive down-regulation of enzymes that allow cell growth but compete for lysine pathway intermediates is a promising approach to further optimize lysine titer (Zhou and Zeng, 2015b). Citrate synthase (encoded by *gltA*) catalyzes lysine-competing consumption of oxaloacetate in the TCA cycle and is a likely target for this approach. A prior DNA-level engineering strategy demonstrated that decreasing transcription of *gltA* by exchanging its native promoter for a low level promoter increases lysine yield but diminishes cell growth (Ooyen et al., 2012). While engineering enzymes for allosteric responsiveness to lysine is possible (Chen et al., 2015), it can be challenging particularly when a crystal structure is not available or when a natural allosteric site is not available as a starting point for engineering. Instead, a lysine-responsive ncRNA riboswitch can offer a more straightforward approach for implementing lysine-dependent expression to any enzyme of choice.

Indeed, a natural lysine-responsive riboswitch upstream of the *lysC* gene in *E. coli* (referred to as RS_{off}) was repurposed in *C. glutamicum* to destabilize the *gltA* mRNA and repress its translation in response to lysine (Caron et al., 2012; Rodionov et al., 2003) (Fig. 2B). The riboswitch was placed in the genome upstream of *gltA* in a strain background that included deregulated *lysC** and *ppc** mutants, which eliminate feedback-inhibition. The riboswitch-containing strain produced 0.23 mol lysine/mol glucose (63% increase from strain lacking RS_{off}) in shake-flask fermentation (Table 1). However, addition of the riboswitch limited biomass accumulation (approximately 20%), likely because endogenous levels of lysine in *C. glutamicum* are capable of repressing *gltA* expression (Zhou and Zeng, 2015b). Results are comparable to the DNA-level strategy: replacing the native *gltA* promoter with a synthetic low-strength promoter increased lysine production by 50% and decreased biomass accumulation by 12% (Ooyen et al., 2012). In future applications, riboswitch sensitivity to lysine could be tuned by mutation and screening to identify variants that could increase lysine productivity apart from decreased growth.

Along these lines, the *E. coli lysC* riboswitch has been used as starting sequence for constructing a synthetic riboswitch that *upregulates* gene expression in response to lysine. After error-prone PCR and screening, the resulting RS_{on} mutant riboswitch was added upstream of *lysE*, a lysine export protein (Fig. 2B) in a *C. glutamicum* genome already harboring the following modifications: *lysC**, *ppc**, and RS_{off} upstream of *gltA*. The *lysE* exporter gene was likely selected as a target to lessen intracellular lysine to help drive flux towards lysine production. This strain produced 0.27 mol lysine/mol glucose in shake-flask fermentation, a 20% increase relative to the strain employing lysine-dependent RS_{off} control of *gltA* described above (Table 1). No additional decrease in cell growth was observed (Zhou and Zeng, 2015a). Taken together, these examples highlight the impact of conditional ncRNA-based gene expression control in pathway engineering. Perhaps combining prior DNA-level strategies that include increased expression of many pathway enzymes (*dapA*, *dapB*, *asd*, *ddh*, and *lysA*) (as in (Ooyen et al., 2012)) with conditional control of *lysE* and *gltA* will allow for further pathway improvements.

Cadaverine, a close derivative of lysine, is a precursor molecule in polyurethane and polyamide syntheses (Qian et al., 2011). While polyamides are typically obtained by petroleum-involved methods, the cadaverine precursor can be produced microbially by overexpression of lysine decarboxylase (Kind et al., 2010; Mimitsuka et al., 2007; Qian et al., 2011) (Fig. 1B). To engineer *E. coli* to overproduce cadaverine, pathway genes have been overexpressed, genes that encode enzymes of competing pathways have been deleted, and native lines of regulation have been eliminated (Qian et al., 2011).

In efforts to further improve yields, asRNA-mediated knockdown of 8 mRNAs that encode cadaverine-competing pathways was pursued: *gltA*, *metB*, *murE*, *murF*, *thrA*, *thrB*, *thrC*, and *thrL* (Fig. 2B) (Na et al., 2013). Targeting *gltA* aimed at limiting competitive consumption of pyruvate and oxaloacetate, while *murE* and *murF* were selected to limit consumption of meso-2,6-diaminopimelate (m-DAP) in peptidoglycan biosynthesis. The remaining targets were selected because they participate in competing consumption of L-aspartate semialdehyde to threonine. An Hfq binding sequence from the *E. coli* MicC sRNA was used a stabilizing scaffold and placed downstream of a 24 nucleotide sequence antisense to the start codon region of each mRNA target. This was done in a strain background already engineered for high cadaverine titer at the DNA level: genes that encode for conversion of

cadaverine to other compounds were deleted (*speE*, *speG*, *puuA*, and *ydjG*) and *cadA* and *dapA* pathway enzymes were overexpressed (Fig. 2B) (Qian et al., 2011). In this genomic background, knockdown of the *murE* mRNA, which converts the immediate precursor of lysine (meso-2,6-diaminopimelate) towards peptidoglycan, best improved cadaverine production. Titer increased to 2.15 g/L in flask culture (Na et al., 2013) from 1.3 g/L in the earlier study that utilized only DNA-level modifications (Qian et al., 2011) (Fig. 2B). In high cell density fed batch fermentation, asRNA knockdown of *murE* increased cadaverine titer by 31% (9.6 g/L without the asRNA to 12.6 g/L with the asRNA) (Table 1).

Importantly, *gltA*, the target repressed by the lysine-responsive RS_{off} riboswitch reviewed above (Zhou and Zeng, 2015b), was investigated as one of 8 mRNA knockdowns to improve cadaverine production. Although diminishing *gltA* activity effectively increased lysine production in the previous examples (Ooyen et al., 2012; Zhou and Zeng, 2015b), it did not affect cadaverine production as compared with the original strain (i.e., no anti-*gltA* sRNA) (Na et al., 2013). This suggests that tuning down *gltA* expression may only affect pathway yield in the presence of other modifications, like deregulation of *lysC, pyc,* or *ppc,* or deletion of *prpC*, which were not applied in the cadaverine example. The comparison also highlights the interdependency of pathway modifications. Given that the effectiveness of one strategy can depend on other pathway modifications, plasmid-based asRNAs are convenient alternatives to genomic deletions for initial studies: they are more easily transferred between different strain backgrounds and can be more easily combined with other strain modifications.

1,3-Diaminopropane (1,3-DAP) has potential uses as a monomer in polyamide production and as a precursor in pharmaceutical production (Chae et al., 2015). However, bacteria natively capable of biosynthesizing 1,3-DAP are pathogenic and offer limited opportunities for industrial-scale production (Chae et al., 2015; Dasu et al., 2006; Ikai and Yamamoto, 1994, 1997). Thus codon-optimized versions of the *dat* and *dcc* genes from *Acinetobacter baumanni*, which catalyze a two-step conversion of L-aspartate 4-semialdehyde (a lysine pathway intermediate) to 1,3-diaminopropane, were overexpressed in *E. coli* (Fig. 2B) (Chae et al., 2015). To enhance heterologous 1,3-DAP biosynthesis, a library of asRNA regulators was designed to knock down mRNA expression of 128 enzymes involved in performing or regulating *E. coli* central carbon metabolism (Chae et al., 2015; Na et al., 2013). These asRNAs were designed as before: a 24 nucleotide sequence antisense to the start codon region of the target mRNA was placed upstream of an Hfq binding scaffold from the MicC sRNA followed by a synthetic terminator (Na et al., 2013). Each asRNA was independently expressed in an *E. coli* strain containing prior DNA-level modifications: *thrA**, *lysC**, and *ppc* and *aspC* overexpression. These served to eliminate native lines of enzymatic feedback-inhibition and to overexpress pathway enzymes (Fig. 2B). Screening revealed several novel pathway engineering targets. In the best case of *pykF* knockdown (i.e., limited conversion of PEP to PYR), titer increased up to 35% (approximately 381 mg/L) in flask culture relative to the control strain that included only the DNA-level modifications (*thrA**, *lysC**, and *ppc* and *aspC* overexpression) (Fig. 2B, Table 1).

Given results obtained via expression of the anti-*pykF* sRNA, genomic deletion of *pykF* in the *thrA**, *lysC**, and *ppc* and *aspC* overexpression strain was explored. Remarkably, genomic deletion of *pykF* did not improve 1,3-diaminopropane titer (Chae et al., 2015). Rather, an intermediate level of *pykF* activity, like that achieved by asRNA-driven knockdown, may be optimal for the 1,3-diaminopropane pathway. This suggests that fine-tuning target mRNA knockdown level (like that done for tyrosine production above) may be a key general strategy for applications of asRNAs.

2.1.3. Putrescine, L-proline, and 5-aminolevulinic acid

Putrescine is naturally produced from α-ketoglutarate via glutamate and ornithine (Fig. 1B). This four-carbon diamine is useful as a monomer in nylon synthesis (Noh et al., 2017; Qian et al., 2009). Glutamate also serves as branch point for the biosynthesis of the amino acid proline and for 5-aminolevulinic acid, a tightly-regulated precursor of heme. This compound has pharmaceutical applications, namely tumor diagnosis and treatment (Peng et al., 1997) and as a biodegradable herbicide (Sasaki et al., 2002). As such, the pathways of these α-ketoglutarate-derived compounds have been engineered by multiple strategies, including ncRNA regulators.

asRNA regulators were applied to the putrescine pathway to precisely down-tune enzyme activity in efforts to optimize titer (Noh et al., 2017). Flux analysis identified nine enzymes for which down-tuned activity would likely impact putrescine productivity: *pfkA*, *pykF*, *aceF*, *poxB*, *sucA*, *aceA*, *glnA*, *proB*, and *gltX*. Six additional enzymes were selected rationally for their involvement in competing or related pathways: *pck*, *pta*, *ackA*, *eno*, *pgi*, and *argF*. Specifically, one asRNA was designed for each target enzyme mRNA. The asRNAs consisted of a sequence antisense to the RBS and start codon regions of the mRNA target, an Hfq-binding scaffold from the *E. coli* SgrS sRNA, and a synthetic terminator. Each asRNA was paired with 5 promoters that represent a range of transcription levels to tune the extent of target enzyme knockdown. In this way, the impacts of 75 conditions on putrescine titer were sampled (Noh et al., 2017). Alternatively, enzyme activity could have been down-tuned by designing multiple asRNAs that each target different portions of a single mRNA to give variable levels of decreased enzyme activity (as in (Na et al., 2013)).

Expression of two asRNAs, anti-*argF* and anti-*glnA*, in a previously engineered putrescine-producing strain (Qian et al., 2009) improved putrescine titer 61% and 25%, respectively, relative to the same strain without asRNA expression (Noh et al., 2017) (Table 1, Fig. 2C). Specifically, this strain contained several genome-level modifications previously demonstrated to improve putrescine titer five-fold: *speE*, *speG*, *argI*, *puuPA*, and *rpoS* are deleted and *argE, argCBH*, *speF-potE*, *argD*, and *speC* are overexpressed from the genome (Qian et al., 2009). It should be noted that *glnA* and *argF* encode pathways that compete with the putrescine pathway for glutamate and ornithine consumption, respectively (Fig. 2C). Importantly, these asRNAs only improved titer when expressed with a weak or medium strength promoter, not the strongest promoter due to negative effects on cell growth rate. Weak expression of *argF* and medium expression of *glnA* increased putrescine titer to 2.7 g/L (61% increase) and 2.1 g/L (25% increase) in flask culture, respectively. In fact, upon combinatorial weak expression of anti-*argF* and medium expression of anti-*glnA*, further down-tuning of asRNA expression level was required due to negative growth rate effects not observed when each was expressed individually. A final 78% increase in putrescine titer to 43 g/L in high cell density fed-batch culture was obtained (relative to the putrescine-producing strain of (Qian et al., 2009) without asRNA expression) (Noh et al., 2017).

It is noteworthy that a similar trend between *argF* expression level, growth rate, and ornithine titer (the immediate putrescine precursor (Fig. 2C)), has also been observed in *C. glutamicum*. In this organism, addition of variable strength transcription terminators just upstream of *argF* in the *argCJBDFR* operon provides a range of decreased *argF* expression levels and reveals an optimal case for maximum ornithine titer (Zhang et al., 2018). These results highlight the value of sampling multiple target enzyme expression levels for pathway optimization, particularly when the target enzymes catalyze key steps in cellular metabolism that can affect growth rate. The ease of doing so with asRNA-mediated knockdown, rather than genomic modification, demonstrates the utility of asRNAs in tuning metabolic routes for pathway engineering. Additionally, the asRNA strategy enabled expression of *argF* to be limited alongside *argI* deletion (Fig. 2C). Deleting *argF* and *argI* in combination produces an impractical arginine auxotrophy in *E. coli* (Qian et al., 2009).

Given the extent of biosynthesis pathway overlap between putrescine and proline (Fig. 1B), the same anti-*argF* and anti-*glnA* sRNA regulators were used to knock down corresponding enzyme activity to

optimize production of proline (Fig. 2C) (Noh et al., 2017). Importantly, this was pursued in an *E. coli* strain background where proline consumption (*putA*), proline import (*puuP*, *putP*, and *proP*), and competing ornithine consumption (*speC*, *speF*) enzymes were deleted and an exogenous ornithine clycodeaminase (*ocd*) from *Pseudomonas putida* was overexpressed by plasmid to directly convert ornithine to proline. Combinatorial expression of the anti-*argF* and anti-*glnA* sRNAs under five variable-strength promoters sampled the impact of 25 conditions on proline titer. Maximum proline titer, 2.02 g/L, was obtained with the anti-*glnA* and anti-*argF* sRNAs expressed under the second strongest and strongest promoters, respectively. This represents a 7-fold increase in proline levels from the same strain lacking asRNA expression (Table 1).

It is remarkable that expressing anti-*glnA* and anti-*argF* with strong promoters provided for optimal proline titer here, while impairing cell growth and reducing titer for putrescine production (Noh et al., 2017). Even though putrescine and proline are both produced in a single step from ornithine, they require different expression levels of *argF*, which competitively consumes ornithine, and *glnA,* which competitively consumes glutamate (Fig. 2C). The observed differences in optimized asRNA expression level between the products reinforce the importance of tailoring pathway modifications for even closely related products. This is made easier with the flexibility of asRNAs to sample and precisely tune levels of decreased enzyme activity.

5-Aminolevulinic acid (5-ALA) is also produced from the α-ketoglutarate and glutamate nodes of *E. coli* central carbon metabolism (Fig. 1B). Importantly, this compound serves as a tightly-controlled step of heme biosynthesis in the cell (Woodard and Dailey, 1995). The global iron-sparing sRNA regulator RyhB represses translation of the enzymes that consume 5-ALA towards heme, as well as several steps of the TCA cycle (Fig. 2C) (Massé et al., 2005). As such, it was hypothesized that overexpressing the RyhB sRNA in an *E. coli* strain background already engineered for 5-ALA production could further increase 5-ALA titers (Li et al., 2014). This background strain is comprised of plasmid-based *hemL*, *hemA** (deregulated mutant of *hemA* from *S. arizona*), and *rhtA* overexpression (Kang et al., 2011). These previously-engineered modifications were executed to (i) overexpress enzymes in efforts to increase pathway flux and (ii) eliminate native enzymatic feedback-inhibition through overexpressing the *rhtA* exporter of 5-ALA and a deregulated mutant of *hemA* (Fig. 2C). Overexpression of the RyhB sRNA regulator increased titer 16% to 1.8 g/L in flask culture (relative to the strain overexpressing *hemL*, *hemA**, and *rhtA* only) (Table 1) (Li et al., 2014).

While only a modest increase in titer, RyhB overexpression elicited a range of expression-level changes to multiple confirmed and some likely mRNA targets. In the RyhB overexpression strain *hemB* and *sdhB* mRNA expression decreased 65%, *cydAB*, *acnAB*, *fumA*, and *sdhA* mRNA expression decreased 30–40%, and *hemH* mRNA expression was nearly fully abolished compared to an *E. coli* strain overexpressing *hemL*, *hemA**, and *rhtA* only (Li et al., 2014). These details highlight how applying a native multi-target sRNA regulator can impact multiple targets to different extents in a coordinated manner to improve a phenotype.

2.1.4. Succinate

Overexpression of the RyhB sRNA regulator has also been applied to engineer succinate production in *E. coli* (Kang et al., 2012). Succinate is an intermediate of the TCA cycle (Fig. 1B) that also functions in oxidative phosphorylation, playing a key role in ATP production. Industrially, succinate is useful as a counter ion in pharmaceutical formulations and as a food additive (Thakker et al., 2011). The RyhB sRNA regulator was expected to be a useful tool for impacting succinate production because it represses expression of the *sdhCDAB*, *fumA*, and *acnAB* mRNAs (Massé et al., 2005; Wang et al., 2015); these catalyze conversion succinate to fumarate, fumarate to malate, and citrate to isocitrate in the TCA cycle, respectively (Fig. 2D). Increased repression of the *sdhCDAB* and *fumA* targets was expected to minimize consumption of succinate. Native sRNA regulator overexpression was coupled with previously-demonstrated genomic deletions of the following genes to rationally optimize flux to succinate via the glyoxylate shunt: *pta*, which competes with the TCA cycle for acetyl-CoA; *poxB*, which competes with acetyl-CoA synthesis for pyruvate; *iclR*, to de-repress *aceAB* expression and activates the glyoxylate shunt; and *ptsG,* to enable arabinose consumption (Fig. 2D) (Kang et al., 2009). In the end, a 5-fold increase in succinate titer was obtained (2.2 g/L) with a 3-fold increase in acetate titer (1.8 g/L) compared to the same strain (Δ*pta*, Δ*poxB*, Δ*iclR*, and Δ*ptsG*) without sRNA overexpression (Table 1) (Kang et al., 2012).

Metabolite measurements support the hypothesis that RyhB targets were affected in a differential yet coordinated manner. Citrate, consumed by the *acnAB*-encoded enzyme, did not accumulate during the experiment, while succinate, consumed by the *sdhAB*-encode enzyme, increased 5-fold. This is in accord with a prior study that suggested RyhB represses *sdhAB* more strongly than *acnAB* (Kang et al., 2012; Massé et al., 2005). Thus, RyhB likely differentially impacts its targets and exerts coordinated control over its native network to improve succinate production.

Other ncRNA approaches have been used to engineer the succinate pathway in *E. coli,* focusing on anaerobic biosynthesis of succinate via hydration of CO_2, carboxylation of PEP to OAA, and subsequent conversion of OAA to malate, fumarate, and succinate (Fig. 2D). One study knocked down *pykF* mRNA expression to limit off-pathway consumption of PEP to PYR, which competes with on-pathway conversion of PEP to OAA (Zhao et al., 2016). Another attempt dynamically controlled heterologously expressed *ecaA* (carbonic anhydrase) and *pepC* (PEP carboxylase) genes from *Anabaena* sp. *7120* in *E. coli* with an activating toe-hold switch system (Wang et al., 2018a). The succinate pathway thus provides a rare example in which the effectiveness of applying single-target ncRNA regulators can be compared with that of a multi-target sRNA regulator in improving product titer. The asRNA and toe-hold switch approaches provided 20% and 13% increases in succinate titer, respectively, relative to their no ncRNA controls, while RyhB overexpression increased succinate titer 5-fold (400%) (Table 1). Although direct comparisons between studies are complicated by differences in growth conditions and genomic differences amongst the strains, overexpression of the RyhB sRNA seemingly better supports increases in succinate production relative to the no ncRNA control than the other ncRNA strategies. The positive impacts of RyhB on 5-ALA and succinate biosynthesis further confirm the potential value of applying native multi-target sRNA regulators to improve production phenotypes.

2.1.5. 6-Deoxyerythronolide B

6-Deoxyerythronolide B (6-DEB) is a polyketide that serves as core component of the antibiotic erythromycin. Naturally biosynthesized in *Saccharopolyspora erythraea*, heterologous overexpression of pathway enzymes in *E. coli* enables 6-DEB expression in the presence of supplied propionate (Pfeifer et al., 2001). The exogenous pathway makes use of native *E. coli* flux through the TCA by consuming succinyl-CoA and exogenously supplied propionate as a second input (Fig. 1B and Fig. 2D). With the aim of increasing conversion, flux analysis was performed to identify suitable but non-intuitive targets for knockdown with asRNAs (Meng et al., 2015). Notably, simulated optimal production conditions were compared with measured transcript levels of an *E. coli* strain expressing the heterologous pathway. Pathway-level discrepancies between actual and simulated conditions revealed that downregulation of the pentose phosphate and nucleotide metabolism pathways may improve 6-DEB titer. As such, 23 mRNA targets from these pathways were selected for knockdown and screening *in vivo*. asRNAs were constructed as before (Na et al., 2013): a 24 nucleotide segment antisense to the target mRNA's start codon and first few codons of coding sequence was placed upstream of an Hfq-biding scaffold repurposed from the MicC sRNA and a strong terminator.

Screening was performed in an *E. coli* background with *prpRBDC*

deleted and *prpE* overexpressed to limit competing propionate consumption and to increase propionate conversion to propionyl-CoA, respectively. Additionally the following non-native enzymes were overexpressed to reconstitute the 6-DEB biosynthesis pathway in *E. coli*: *eryAI*, *eryAII*, and *eryAIII* from *S. erythraea*, *pccB* and *accA2* from *S. coelicolor*, and *sfp* from *B. subtilis* (Fig. 2D). The *pccB* and *aacA1* genes together encode propionyl-CoA carboxylase, which enables reaction of propionyl-CoA to (2S)-methylmalonyl-CoA (Boghigian Brett et al., 2011). The *eryAI-III* genes together encode deoxyerythronolide B synthase (DEBS), which combines one propionyl-CoA molecule with 6 molecules of (2S)-methylmalonyl-CoA to synthesize 6-DEB (Pfeifer et al., 2001). Finally, *sfp* (phosphopantetheinyl transferase) provides function-critical post-translational modification of DEBS (Pfeifer et al., 2001). Results revealed that knockdown of nearly all targets improved 6-DEB titer. Pairing the best asRNAs together for combinatorial expression demonstrated that dual knockdown of *guaB* and *zwf*, which convert IMP to GMP and catalyze the first step of the pentose phosphate pathway, respectively, can boost titers to 210 mg/L, a nearly 4-fold increase from the control strain (i.e. no asRNA expression) in flask culture (Meng et al., 2015) (Table 1). This reinforces how flux analysis can be used to identify promising asRNA knockdown targets that, with screening, can effect substantial impacts on pathway titer. It also demonstrates the informative role omics datasets can play in guiding selection of mRNAs to target with asRNA knockdown.

2.2. Flux through Malonyl-CoA and Acetyl-CoA

Malonyl-CoA and acetyl-CoA play a role in multiple metabolic pathways in bacteria. In addition to serving as a precursor for the TCA cycle, acetyl-CoA is consumed in the biosynthesis of fatty acids and isoprenoids, like amorphadiene. Malonyl-CoA is synthesized from acetyl-CoA and is consumed in fatty acid biosynthesis. It also provides for the synthesis of more complex compounds, like 4-hydroxycoumarin, resveratrol, and (2S)-naringenin (Fig. 1B, Fig. 3A). What is common among these valuable end products is that the bacteria or plants that naturally synthesize them are not viable or sustainable at an industrial scale (Hale et al., 2007; Yang et al., 2015). As such, *E. coli* has been used as a chassis organism for their heterologous production and, as illustrated with 6-DEB, native metabolism needs tuning to best support production of complex exogenous compounds. ncRNA-based engineering strategies have found application and success in this area. Multiple fatty acid biosynthesis genes have been targeted by asRNA knockdown to increase accumulation of malonyl-CoA and production of downstream, exogenous compounds: 4-hydroxycoumarin, resveratrol, and (2S)-naringenin (Fig. 3A). These studies showcase how a single ncRNA strategy can support production of multiple products along a pathway. Additionally, they demonstrate that using a single native sRNA regulator can support a complex phenotype, one that might require multiple asRNA knockdowns to achieve.

2.2.1. Malonyl-CoA

Studies have aimed to decrease metabolic flux into fatty acid biosynthesis to increase accumulation of malonyl-CoA in *E. coli* as a first step in synthesizing more complex, exogenous products. To this end, *fabB, fabF* and *fabD,* involved in acyl-acyl carrier protein (ACP) transfer reactions in fatty acid biosynthesis, have been identified as useful targets (Wu et al., 2014; Yang et al., 2015) (Fig. 3A). Simultaneous knockdown of *fabB* and *fabF* was expected to increase malonyl-CoA titer because addition of cerulenin, an expensive antibiotic, inhibits *fabB*- and *fabF*-encoded beta-ketoacyl ACP synthases and increases naringenin titer (Davis et al., 2000; Leonard et al., 2008; Santos et al., 2011; Wu et al., 2014). In a second study, *fabD* was selected as a viable target because it catalyzes transfer of malonyl from malonyl-CoA to malonyl-ACP, propelling fatty acid biosynthesis (Yang et al., 2015) (Fig. 3A). Because genomic deletions of fatty acid biosynthesis genes tend to inhibit cell growth (Magnuson et al., 1993), asRNA-mediated knockdown offers a viable approach to manipulate these genes.

In both studies, paired-termini antisense RNAs (PTasRNAs) were built to knock down *fabB*, *fabF* and *fabD*. PTasRNAs employ synthetic base-pairing 5′ and 3′ termini sequences rather than an Hfq-binding scaffold to stabilize the synthetic construct (Fig. 1A II). In these examples, PTasRNAs were constructed by placing synthetic base-pairing 5′ and 3′ termini up and downstream of segments antisense to each mRNA target of interest. By varying the length and position of the targeted region within each target mRNA, Wu and colleagues effectively sampled a range of *fabB* and *fabF* knockdown levels for malonyl-CoA accumulation. Screening the library of PTasRNAs revealed that pairing the *fabF*-targeting and *fabB*-targeting PTasRNAs with the highest knockdown activities (~80% decrease in target enzyme activity) provided maximum malonyl-CoA titer: 0.88 nmol/mg DCW (8.8-fold increase relative to wild type, which lacks the PTasRNAs) (Wu et al., 2014). For the case of *fabD* knockdown, an antisense segment that decreased *fabD* mRNA expression ~70% was ultimately used; it provided 0.25 nmol/mg DCW malonyl-CoA, a 4.5-fold increase in titer compared to the wild type strain, which lacks the PTasRNA (Table 1) (Yang et al., 2015).

Direct comparison between the efficacy of *fabB* and *fabF* versus *fabD* knockdowns in increasing malonyl-CoA titer is complicated by differences in growth conditions between the studies. Titer was measured after 48 h for the anti-*fabB* and anti-*fabF* PTasRNAs, while it was measured after 12 h for the anti-*fabD* PTasRNA (Table 1). Based on the available information, combinatorial knockdown of *fabB* and *fabF* seemingly better supports malonyl-CoA accumulation than *fabD* knockdown compared to the control cases (8.8-fold versus 4.5-fold increase). This difference in efficacy was seemingly conserved when each strategy was applied to production of (2S)-naringenin, a malonyl-CoA-derived flavonoid compound that serves as platform for synthesis of other flavonoids and may have benefits as a pharmaceutical (Fig. 1B) (Leonard et al., 2008; Santos et al., 2011) (Table 2). The same asRNA strategies pursued in Wu et al. and Yang et al. for malonyl-CoA production were applied to improve (2S)-naringenin titer because improved malonyl-CoA accumulation was expected to drive increases in titer of products downstream in the pathway (Fig. 3A).

The *anti-fabB* and *anti-fabF* PTasRNAs were overexpressed with the following exogenous (2S)-naringenin pathway enzymes in the presence of 3 mM added tyrosine and 2 g/L added malonate: tyrosine ammonia lyase (TAL) from *Rhodotorula glutinis*, converts tyrosine to p-coumaric acid; 4-coumarate-CoA ligase (4CL) from *Petroselinum crispum*, ligates CoA to p-coumaric acid to yield coumaroyl-CoA; chalcone synthase (CHS) from *Petunia hybrida*, condenses 4 coumaroyl-CoA and 3 malonyl-CoA molecules to form naringenin chalcone; and chalcone isomerase (CHI) from *Medicago sativa*, catalyzes a ring closure reaction to produce (2S)-naringenin. The *matB* and *matC* genes from *Rhizobium trifoli* were also included to supplement native *E. coli* malonyl-CoA production with production from the added malonate (Fig. 3A). The library of PTasRNAs that provided a range of *fabF* and *fabB* knockdown were tested again; application of the PTasRNAs that gave greatest *fabB* and *fabF* knockdown level (~80%) and malonyl-CoA titer did not maximize (2S)-naringenin titer. Rather, overexpression of the PTasRNAs that gave intermediate knockdown levels of *fabB* and *fabF* (~50%) resulted in 391 mg/L (2S)-naringenin, a 4.3-fold increase compared to the control strain harboring only the exogenous pathway (Table 1) (Wu et al., 2014). Similarly, Yang et al. paired their anti-*fabD* PTasRNA with a pathway that synthesizes (2S)-naringenin from malonyl-CoA and added 1 mM p-coumaric acid: 4-coumarate: CoA ligase (4CL) from *Petroselinum crispum*, chalcone synthase (CHS) from *Petunia hybrida*, and chalcone isomerase (CHI) from *Medicago sativa.* This provided 91.3 mg/L (2S)-naringenin, a 50% increase from the control strain lacking only the anti-*fabD* PTasRNA (Table 1) (Yang et al., 2015). The anti-*fabD* PTasRNA was also used to improve heterologous expression of 4-hydroxycoumarin and resveratrol in *E. coli*. Similar to (2S)-naringenin, these compounds are synthesized from malonyl-CoA

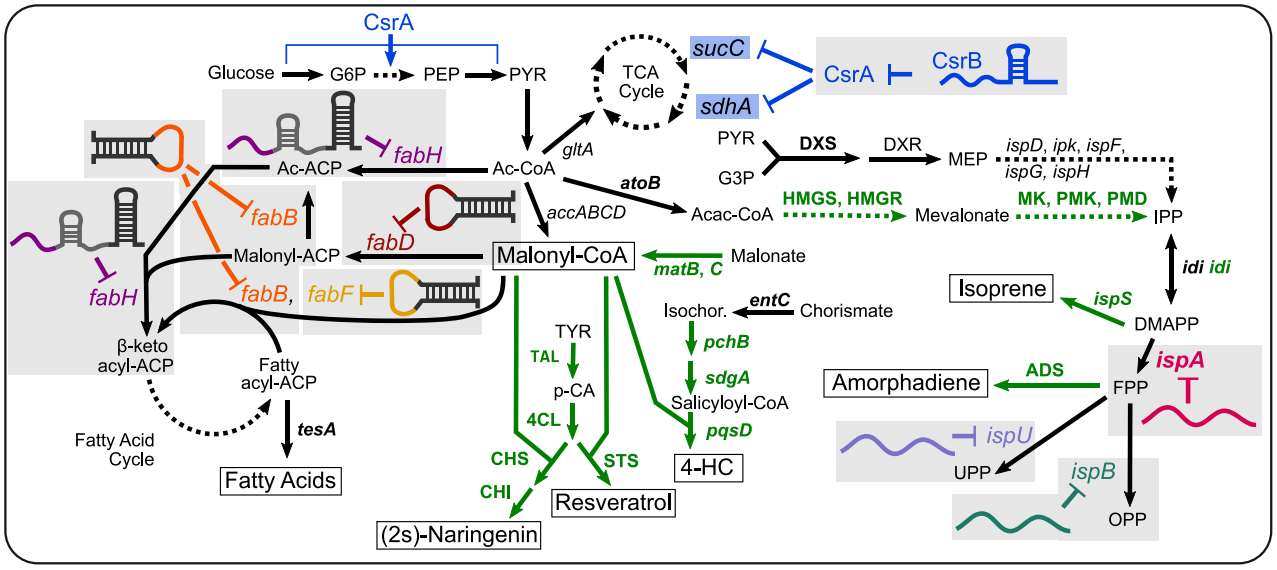

(caption on next page)

Fig. 3. Other pathways and phenotypes engineered with ncRNAs. Pathway diagrams include solid arrows to indicate single enzymatic steps and dashed arrows to indicate multiple enzymatic steps. Boxed, large type compounds are overproduced by an ncRNA-based pathway engineering strategy. asRNA, PTasRNA, long asRNA and native sRNA icons from Fig. 1A are used to indicate the type of ncRNA tool and target(s). Other pathway engineering strategies used with the ncRNA-based strategy are depicted: gene overexpression (**bold type**), exogenous gene overexpression (**green bold type**), enzyme de-regulation mutations (*), and gene deletion (red circle-line "not" symbol). (A) Production of malonyl- and acetyl-CoA-derived products is supported by asRNA, PTasRNA, and long asRNA-mediated knockdown of fatty acid and isoprene biosynthesis genes and overexpression of the native CsrB sRNA. Genes shaded blue are regulated at the mRNA level by CsrA, which is sequestered by CsrB. Activation of glycolysis enzymes by CsrA is shown by a blue arrow and bracket (direct interactions not fully confirmed). (B) Alcohol production and tolerance is driven by ncRNA-based engineering strategies. CsrB and 6S sRNA overexpression as well as knockdown of key competing lactate, acetate, 2,3-butanediol, or 1,3-propanediol production mRNAs, support butanol and ethanol production in *E. coli*, *C. acetobutylicum*, *C. pasteurianum,* and *K. pneumoniae*. asRNA knockdown also enriches 1,3-propanediol and 1,3-hydroxypropionic acid production in *K. pneumoniae.* (C) Acid resistance phenotype can be supported by native sRNA overexpression. DsrA, RprA, and ArcZ sRNA overexpression improves acid tolerance in *E. coli* by activing RpoS and downstream acid resistance mechanisms. (D) The doxorubicin pathway in *S. peucetius* is improved by PTasRNA-mediated knockdown of the DoxR transcription factor, thus activating the DnrI transcription factor and transcription of DXR biosynthesis genes. (E) GlcNAc production in *B. subtilis* is enriched with anti-*pfk* and anti-*glmM* sRNAs, which impede glycolysis (*pfk*) and peptidoglycan biosynthesis (*glmM*), respectively. Abbreviations are as follows: G3P, glyceraldeyde-3-phosphate; G6P, glucose-6-phosphate; PEP, phosphoenol pyruvate; PYR, pyruvate; Ac-CoA, acetyl-CoA; Ac-ACP, acetyl-ACP; Acac-CoA, acetoacetyl-CoA; MEP, methylerythritol 4-phosphate; IPP, isopentenyl diphosphate; DMAPP, dimethylallyl diphosphate; FPP, farnesyl diphosphate; UPP, undecaprenyl diphosphate; OPP, octaprenyl diphosphate; DHA, dihydroxyacetone; 3-HPA, 3-hydroxypropionaldehyde; 1,3-PDO, 1,3-propanediol; 3-HP, 3-hydroxypropionic acid; 3-HB-CoA, 3-hydroxybutryl-CoA; 2,3-BDO, 2,3-butanediol; FeDox-ox, oxidized ferroredoxin; FeDox-red, reduced ferroredoxin; AA AR, amino acid resistance; DXR, doxorubicin; G1P, glucose-1-phosphate; TDP, thymidine diphosphate; GlcN-6P, glucosamine-6-phosphate; GlcN-1P, glucosamine-1-phosphate; GlcNAc-6P, N-acetylglucosamine-6-phosphate; GlcNAc, N-acetyl-glucosamine.

(Fig. 3A). The PTasRNA provided 271 mg/L 4-hydroxycoumarin and 268 mg/L resveratrol, 2.5-fold and 70% increases, respectively, from the control strains expressing the heterologous pathways only (Table 1) (Yang et al., 2015).

The (2S)-naringenin pathway heterologously expressed in *E. coli* has also been engineered using the clustered regularly interspaced short palindromic repeats interference (CRISPRi) approach (Wu et al., 2015). CRISPRi makes use of small guide RNAs, bound to a deactivated Cas9 protein, to repress transcription of a target gene at the DNA level (Bikard et al., 2013; Gilbert et al., 2013; Konermann et al., 2013; Qi et al., 2013; Zhao et al., 2014). Like asRNA knockdown, this technique is promising for its ability to allow easier exploration of gene repression combinations relative to traditional genetic deletion approaches (Choi and Lee, 2016; Doudna and Charpentier, 2014; Hsu et al., 2014; Wang et al., 2016a). Here, repression of 30 genes in central carbon metabolism and fatty acid biosynthesis was screened for impact on malonyl-CoA accumulation. Importantly, CRISPRi screening also revealed *fabB* and *fabF* as promising targets. Promising CRISPRi targets were expressed alongside the exogenous (2S)-naringenin pathway described for (Wu et al., 2014) above; however, supplementary malonate and accompanying *matB* and *matC* genes from *Rhizobium trifoli* were not included. Dual repression of the *fabB* and *fabF* genes increased (2S)-naringenin titer approximately 3-fold at 48 h of growth (Wu et al., 2015), remarkably similar to the 4.3-fold increase in (2S)-naringenin titer achieved with the anti-*fabB* and anti-*fabF* PTasRNAS (Wu et al., 2014).

It should be noted that Yang and colleagues also mapped the effect of antisense knockdown of *fabH*, *fabB*, and *fabF* in their system (Yang et al., 2015). They observed substantial sensitivity of 4-hydroxycoumarin titer to the regions of *fabB* and *fabF* that were targeted by PTasRNA. Similar to the observation made by (Wu et al., 2014) in optimizing naringenin production, Yang et al. found that a middle level of *fabB* and *fabF* expression was best for 4-hydroxycoumarin production (Yang et al., 2015). However, the anti-*fabD* PTasRNA still performed better in their system than the anti-*fabF* and anti-*fabB* PTasRNAs. This is likely due to differences in growth conditions between the two studies (Table 1) or to differences in how the exogenous pathway was reconstituted in *E. coli*. Overall, these studies reiterate the usefulness of fine-tuning enzyme knockdown levels via asRNA strategies for maximum pathway improvement. It is also worth mentioning that supplementing cultures with tyrosine or p-coumarate was required for exogenous (2S)-naringenin and resveratrol biosynthesis in *E. coli* (Wu et al., 2014; Yang et al., 2015). Applying the anti-*csrA* and anti-*tyrR* sRNAs used to improve tyrosine production (Na et al., 2013) may minimize the need to add tyrosine or p-coumarate to support synthesis of the (2S)-naringenin and resveratrol polyketides in *E. coli*.

2.2.2. Acetyl-CoA

Other studies have focused on applying native ncRNAs to accentuate fatty acid biosynthesis, rather than directing flux away from it. For example, the CsrB sRNA has been overexpressed in *E. coli* to improve long-chain fatty acid biosynthesis (McKee et al., 2012). Specifically, CsrB was identified as tool for pathway engineering based on the breadth of its effects on central carbon metabolism: overexpression of CsrB increases glycogen biosynthesis (Liu et al., 1997), gluconeogenesis (Romeo et al., 2013; Vakulskas et al., 2015), biofilm formation (Wang et al., 2005) and accumulation of phenylalanine (Yakandawala et al., 2008). It is understood that these impacts stem from CsrB antagonizing the direct target binding interactions of the CsrA global RNA binding protein regulator (Sowa et al., 2017; Vakulskas et al., 2016). As a first step to using CsrB as a pathway engineering tool, the impact of CsrB overexpression on metabolism was mapped by proteomics and metabolomics in an *E. coli* background auxotrophic for phenylalanine and isoleucine (*E. coli* BLR with further Δ*tyrR*, Δ*pheA/L*, *aroF** and *tyrA** genetic modifications). Results demonstrated that CsrB alters expression of central carbon metabolism, TCA cycle, and pentose phosphate pathway proteins and that it substantially alters accumulation of amino acids and TCA cycle-related compounds (McKee et al., 2012). Since this study, a number of new directly repressed targets of CsrA have been characterized, including the *sucC* and *sdhA* mRNAs (Fig. 3A), which support the effect of CsrB on flux through the TCA cycle (Sowa et al., 2017).

Notably, acetyl-CoA accumulation increased 8-fold upon CsrB overexpression (compared to the BLR Δ*tyrR*, Δ*pheA/L*, *aroF** and *tyrA** *E. coli* strain lacking CsrB overexpression) (McKee et al., 2012). Rather than pursuing extensive genome engineering to obtain a similar increase in acetyl-CoA levels, McKee and colleagues overexpressed CsrB and the *tesA* gene in *E. coli* to improve its native fatty acid biosynthetic capabilities; *tesA* encodes for an enzyme that generates free fatty acids and fatty esters from actively elongating fatty acid chains by cleaving off their acyl-ACP groups. This provided 430 mg/L long fatty acids, an 85% increase from the control strain (BLR Δ*tyrR*, Δ*pheA/L*, *aroF** and *tyrA** strain expressing *tesA* but lacking CsrB overexpression) (Table 1) (McKee et al., 2012).

Importantly, McKee et al. extended this approach to heterologous production of amorphadiene in *E. coli* (Martin et al., 2003), an isoprenoid precursor of the valuable antimalarial artemisinin (Dhingra et al., 1999). Typically found in the leaves of *Artemisia annua*, extraction of amorphadiene and related terpene compounds is inefficient (Martin et al., 2003). Thus, microbial biosynthesis is desirable. *E. coli* natively produces the isoprenoid precursors isopentenyl diphosphate (IPP) and dimethylallyl diphosphate (DMAPP) by the methylerythritol 4-phosphate (MEP) pathway. This isoprenoid pathway branches off

from *E. coli* central carbon metabolism at glyceraldehyde-3-phosphate and pyruvate (Fig. 3A). However, to bypass native regulation, the mevalonate-dependent isoprenoid pathway from *S. cerevisiae*, which branches off of central carbon metabolism at acetyl-CoA, was reconstituted in *E. coli* (Martin et al., 2003). As such, overexpression of CsrB was expected to support increases in amorphadiene titer in the current work (McKee et al., 2012). The following pathway genes were overexpressed with the CsrB sRNA: *atoB* (*E. coli*), condenses two acetyl-CoA molecules into acetoacetyl-CoA; HMGS (*S. cerevisiae*), synthesizes 3-hydroxy-3-methyl-glutaryl-CoA (HMG-CoA) from acetyl-CoA and acetoacetyl-CoA; HMGR (*D. acidovorans*), reduces HMG-CoA to mevalonate; MK (*S. cerevisiae*), mevalonate kinase; PMK (*S. cerevisiae*), phosphomevalonate kinase; PMD (*S. cerevisiae*), decarboxylates pyrophosphomevalonate to IPP; *idi* (*E. coli*), IPP-DMAPP isomerase; *ispA* (*E. coli*), synthesizes farnesyl diphosphate (FPP) from DMAPP; and ADS (*Artemisia annua*), synthesizes amorphadiene by a ring closure of FPP. Co-overexpression of CsrB with this pathway provided 93 mg/L amorphadiene, a 55% increase compared to the control strain (BLR Δ*tyrR*, Δ*pheA/L*, *aroF** and *tyrA** overexpressing the pathway but lacking CsrB overexpression) (McKee et al., 2012).

Remarkably, overexpressing the CsrB sRNA supported increases in biosynthesis of fatty acids and a complex product derived from acetyl-CoA. This suggests that the predominant impact of CsrB overexpression for improving fatty acid and amorphadiene production is upstream of the acetyl-CoA branch point of the two pathways (Fig. 3A); based on these results, overexpression of CsrB would likely support increased titers of malonyl-CoA-derived compounds as well. Importantly, these CsrB examples contrast the examples where fatty acid biosynthesis genes like *fabF*, *fabB*, and *fabD*, were knocked down by asRNAs to decrease competing malonyl-CoA consumption and improve the titers of malonyl-CoA derived products, like (2S)-naringenin, 4-hydroxycoumaric acid, and resveratrol. The comparison highlights the versatility of using native sRNA regulators to elicit multi-faceted effects to support related pathways.

2.3. Alcohol biosynthesis and tolerance

Microbial synthesis of alcohols like butanol and ethanol has garnered much interest in the biofuel community. In this area, bacteria with naturally high alcohol production and alcohol tolerance levels serve as model strains. While pathways within these organisms can be imported into the classic *E. coli* chassis strain (McKee et al., 2012), these organisms have also been engineered to further enhance their native alcohologenic phenotypes. For example, *Clostridium acetobutylicum* and related species have been engineered for improved 1-butanol titers (Lee Sang et al., 2008; Lütke-Eversloh and Bahl, 2011). Additionally, works have focused on limiting the formation of byproducts, like acetate and lactate, to redirect cellular resources towards desired 1-butanol and ethanol end products (Li et al., 2012b; Lütke-Eversloh and Bahl, 2011). Importantly, ncRNA-based strategies have been applied to engineer the 1-butanol and ethanol pathways in *Clostridium* species and the 1-butanol pathway heterologously expressed in *E. coli* (Table 1). These studies highlight the challenges of tuning complex phenotypes. Furthermore, while native sRNA regulators have been used to support improvements in alcohol related productivity, a lack of understanding of the regulatory and tolerance mechanisms involved hamper future advances.

2.3.1. 1-Butanol

1-Butanol is valuable for its applications as a biofuel. In *Clostridium acetobutylicum*, the 1-butanol pathway diverges from central carbon metabolism at the acetyl-CoA branch point. Four steps convert acetyl-CoA to butyryl-CoA and two subsequent dehydrogenation steps produce 1-butanol (Fig. 3B) (Lee Sang et al., 2008; Lütke-Eversloh and Bahl, 2011). Given the success of overexpressing CsrB in *E. coli* for improved titers of acetyl-CoA and malonyl-CoA derived products, CsrB was overexpressed in *E. coli* in the presence of the imported 1-butanol pathway from *C. acetobutylicum* (McKee et al., 2012). Specifically, *hbd*, *crt*, *bcd, eftAB*, and *adhE2* of *C. acetobutylicum* were overexpressed with a native *E. coli* acetyl-CoA acetyltransferase gene, *atoB,* with and without the CsrB sRNA in an *E. coli* BLR strain containing Δ*tyrR*, Δ*pheA/L*, *aroF** and *tyrA** modifications (isoleucine and phenylalanine auxotrophic background). Briefly, the heterologous genes enable reduction of acetoacetyl-CoA (made by acetylation of acetyl-CoA via *atoB*) to 3-hydroxybutanoyl-CoA (*hbd*), dehydration of 3-hydroxybutanoyl-CoA to crotonyl-CoA (*crt*), hydrogenation of crotonyl-CoA to butyryl-CoA (*bcd* with *eftAB*-encoded flavoproteins), and two sequential hydrogenation steps to yield 1-butanol (*adhE*2). Inclusion of the global sRNA regulator prompted an 88% increase in 1-butanol titer up to 90 mg/L most likely by increasing the pool of available acetyl-CoA to drive flux through the exogenous pathway (McKee et al., 2012).

Unfortunately, the CsrB sRNA regulator holds little potential for engineering the 1-butanol pathway within its native *C. acetobutylicum* host. Even though the Csr/Rsm system is conserved across many organisms and *C. acetobutylicum* does contain CsrA and CsrB homologs (Finn et al., 2016; Romeo, 1998), substantial differences in Csr regulators and target scope exist between gram negative and gram positive bacteria (Vakulskas et al., 2015). As such, alternative sRNA regulators need to be considered to pursue a similar strategy for 1-butanol pathway engineering in *C. acetobutylicum*. One study focused on the 6S sRNA because of its established stress-responsive behavior (Cavanagh et al., 2012; Jones et al., 2016; Venkataramanan et al., 2013). In particular, the 6S RNA binds and sequesters the RNA polymerase-housekeeping sigma factor (sigma70) complex to allow transcription of genes dependent on other sigma factors (i.e., stress response) (Cavanagh et al., 2012). As such, it has been hypothesized that overexpression of the 6S sRNA would increase 1-butanol tolerance and titer (Fig. 3B).

Overexpression of the 6S RNA in the wild type ATCC 824*C. acetobutylicum* strain increased 1-butanol titer 20% to 180 mM (13.3 g/L) and consistently improved *C. acetobutylicum* survival under 1-butanol stress (1–2% v/v) relative to the wild type strain without 6S sRNA overexpression (Table 1) (Jones et al., 2016). Importantly, titer of the *C. acetobutylicum* 1-butanol pathway in its native host is approximately 100-fold greater than that of the pathway imported into *E. coli* (13.3 g/L in Jones et al. versus 0.09 g/L in McKee et al.). The discrepancy in 1-butanol productivity between source *C. acetobutylicum* and host *E. coli* organisms exemplifies the motivation to improve characterization of biotechnologically relevant source organisms. Pathway engineering in the source organism can make use of natural product tolerance mechanisms lacking in the host organism. In general, sRNA characterization lags behind that of protein-coding sequences in these non-model organisms. For the case of *C. acetobutylicum*, 159 sRNAs have been identified from transcriptomics data and expression has been confirmed by northern blot or qRT-PCR for approximately 40 sRNAs (Chen et al., 2011a; Venkataramanan et al., 2013). However, little is known about the specific functions of the sRNAs (Jones et al., 2018). One exception to this rule is the *solB* sRNA. It has been reported to likely repress expression of an operon involved in solventogenesis (Venkataramanan et al., 2013). However, exposure to 1-butanol stress triggers non-intuitive expression level changes of the putative targets of this regulator, suggesting that other regulators may be involved (Venkataramanan et al., 2013). Additionally, *solB* deletion causes unexpected decreases in titer (Jones et al., 2018), rendering this sRNA an impractical tool for engineering 1-butanol synthesis and tolerance. As such, characterization of more sRNAs in non-*E. coli* systems like *C. acetobutylicum* holds potential for future advances in engineering the complex phenotype of alcohol biosynthesis and tolerance.

Targeted asRNA knockdown strategies have also been applied to engineer 1-butanol production. In *Clostridium pasteurianum*, the *hydA* gene was knocked down with the goal of improving titer of 1-butanol (Pyne et al., 2015). *C. pasteurianum* differs from *C. acetobutylicum* in its ability to grow on glycerol, converting it to 1,3-propanediol or to

glycerol-3-phosphate for use in glycolysis. This is an attractive quality because large amounts of glycerol are generated as byproducts of biodiesel production (Yang et al., 2012; Yazdani and Gonzalez, 2007). The *hydA* gene encodes a ferredoxin hydrogenase that converts ferredoxin from its reduced to its oxidized state. This in turn facilitates ferrodoxin-dependent conversion of pyruvate to acetyl-CoA and ferrodoxin-dependent conversion of NADPH and NADH to their opposite oxidation states (Schwarz et al., 2017) (Fig. 3B). Importantly, the NADH-NAD + redox balance is known to influence relative fluxes towards acidic compounds, like acetate, butyrate, and lactate, and solvent compounds, like butanol and ethanol in solventogenic bacteria (Wietzke and Bahl, 2012).

Knockdown of *hydA* was expected to increase intracellular levels of reduced cofactors to favor production of reduced alcohols, like 1-butanol. A long asRNA regulator was constructed to knockdown *hydA* by placing a 175 nucleotide-long sequence complementary to the RBS and the first 164 nucleotides of the coding sequence of *hydA* on a plasmid downstream of a strong promoter and upstream of a strong terminator. Overexpression of the anti-*hydA* long asRNA in wild type *C. pasteurianum* ATCC 6013 provided a 12% increase in 1-butanol titer to 10 g/L, while decreasing 1,3-propanediol titer 30% (3.3–2.3 g/L), relative to wild type *C. pasteurianum* without long asRNA expression. In addition, this approach remodeled metabolic flux to alter titers of pathway intermediates and other byproducts: butyrate titer increased 40% to 0.21 g/L, ethanol titer increased 25% to 2.0 g/L, and acetate titer increased 137% to 0.90 g/L. Strong increases in acidic compounds counter the original hypothesis, indicating that the impact of *hydA* on cellular metabolism is more complex than anticipated (Pyne et al., 2015). More broadly, for complex phenotypes like alcohol biosynthesis, targeting single enzymes for knockdown can result in a trial and error process, urging more clear understanding of the bigger regulatory picture that affects these pathways.

2.3.2. Ethanol

Some *Clostridium* species, like *C. cellulolyticum,* are natively suited for ethanol production. *C. cellulolyticum* has received interest for its ability to hydrolyze cellulose, a step typically accomplished by addition of external cellulases, and for its ability to produce lactate, acetate, and ethanol during fermentation (Desvaux, 2005). Ethanol is the most valuable product of this set, likely for its biofuel applications (Xu et al., 2017). It is synthesized from acetyl-CoA by a bifunctional aldehyde and alcohol dehydrogenase (*adhE*) (Fig. 3B). As such, pathway engineering has focused on minimizing competing consumption of pyruvate to lactate and acetyl-CoA to acetate. Although lactate synthesis can be addressed by genomic deletions of two key hydrogenase genes, *ldh* and *mdh*, genes that encode enzymes for acetate synthesis, *pta* and *ack*, are likely essential and cannot be deleted (Li et al., 2012b). As such, long asRNAs were designed to bind and knock down translation of the *pta* and *ack* mRNAs. The asRNAs were each complementary to a large portion of their target mRNA, which spanned the 5′ UTR, RBS, start codon, and approximately the first 120 nucleotides of coding sequence of the target mRNA. However, only the anti-*pta* long asRNA knocked down enzyme activity (35%). Plasmid overexpression of this long asRNA in a *C. cellulolyticum* background lacking *ldh* and *mdh* effectively (i) maintained minimal lactate production, (ii) limited production of acetate, and (iii) improved ethanol titer. Specifically, negligible lactate (2 ± 8 mg/L), 0.5 g/L acetate (33% decrease), and 1.96 g/L ethanol (86% increase) were quantified for the *C. cellulolyticum* strain expressing the anti-*pta* sRNA after growth in 10 g/L cellulose (relative to the *C. cellulolyticum* Δ*ldh* and Δ*mdh* strain lacking the long asRNA) (Xu et al., 2017).

These results highlight the utility of asRNAs to knockdown competing, essential pathways that are inaccessible by genomic deletion. It should be noted, however, that expression level of the anti-*pta* long asRNA played a large role in the efficacy of the knockdown strategy for improving ethanol titer, implying that fine-tuning of asRNA expression and/or asRNA knockdown efficacy could further aid pathway engineering for optimized ethanol production. Genomic integration of the anti-*pta* long asRNA such that the natural promoter of *adhE* (aldehyde and alcohol dehydrogenase gene) drove its expression was insufficient to consistently decrease acetate titer (Xu et al., 2017). Rather, a similar result in acetate titer was observed only when the anti-*pta* long asRNA was integrated into the genome with a strong synthetic promoter that was comparable in expression level with the promoter of the plasmid system.

2.4. Acid resistance and tolerance phenotypes

Another stress that is of interest to the microbial engineering community is exposure to acidic conditions, as accumulation of cell growth byproducts (like acetate) can limit growth; this is a particular challenge in high cell density fermentations used to overproduce engineered products. Given the multiple complex mechanisms and diffuse regulation involved in the phenotype (Kanjee and Houry, 2013), pathway engineering targets are not as obvious as they tend to be for a standard metabolic product.

For example, *E. coli* natively exhibits acid tolerance by several mechanisms (Fig. 3C). One set of mechanisms couples proton consumption with glutamate, lysine, and arginine decarboxylation. These modified amino acids are then exported in exchange for an unmodified copy of the amino acid from the environment (Foster, 2004). In stationary phase, the *E. coli* RpoS sigma factor mediates expression of an ATPase that couples ATP consumption with proton export (Gaida et al., 2013). RpoS also influences the amino acid-linked mechanisms by mediating expression of their upstream regulators (Battesti et al., 2011). Another player in this system is the H-NS protein, which downregulates RpoS and several up-regulators of the amino acid-linked mechanisms (Krin et al., 2010) (Fig. 3C). Importantly, several sRNAs are known to upregulate translation of RpoS at the mRNA level: DsrA, RprA, and ArcZ. Additionally, the DsrA sRNA downregulates translation of the H-NS protein (Lease and Belfort, 2000).

This vast regulatory system makes many pathways available for engineering intervention. One study hypothesized that overexpression of the DsrA, RprA, and ArcZ sRNAs would upregulate the acid resistance mechanisms in a multi-faceted manner to improve acid stress survival (Gaida et al., 2013). Indeed, overexpression of each sRNA (DsrA, RprA, and ArcZ) increased the survival of K-12 MG1655 *E. coli* under a pH 2.5 acid stress applied during late exponential growth phase: RprA increased survival 3-fold, ArcZ increased survival 5-fold, and DsrA increased survival 106-fold relative to the wild type strain (Table 1). Remarkably, overexpressing all three sRNAs in combination provided for 8500-fold greater survival. This supra-additive impact is particularly revealing when considered with the fact that RpoS overexpression only increases survival approximately 50-fold (Gaida et al., 2013). Results illustrate the complexity of resistance phenotypes: increasing RpoS expression with its native regulators effectively exploits a multi-regulator phenotype inaccessible by direct overexpression of RpoS (Gaida et al., 2013). To our knowledge, this study represents one of the first attempts to overexpress multiple native sRNA regulators to influence a phenotype; it illustrates that overexpressing native sRNA regulators that naturally co-regulate a desired complex phenotype can coherently impact multiple targets to impact phenotype in a coordinated manner.

Importantly, the DsrA, ArcZ, and RprA sRNAs used above had been previously identified and characterized as regulators of RpoS, which had already been implicated in the acid resistance phenotype. However, this level of understanding is not always available for biotechnologically relevant organisms. Moreover, limited numbers of sRNAs have been identified and confirmed in these organisms. As such, groups have worked to develop transcriptomic and bioinformatic approaches to identify sRNAs and their potential targets (Li et al., 2012a; Sharma and Vogel, 2014) (discussed in detail in Section 3); future interests lie in

identifying sRNA regulators with mRNA target networks *relevant to a desired phenotype* for immediate application in pathway engineering. Along these lines, Cho et al. looked to identify and confirm expression of ethanol-responsive sRNAs in *Zymomonas mobilis,* a bacterium natively tolerant and suited to ethanol production (Wang et al., 2018b; Yang et al., 2016b). Transcriptome-wide sequencing data obtained in low and high ethanol conditions were analyzed, compared, and used to identify likely ethanol stress-responsive sRNAs. Northern blots confirmed expression of 15 sRNAs and revealed 4 sRNA regulators that were differentially expressed in the presence of ethanol (Cho et al., 2014). Overexpression of these sRNAs may provide for future improvements in ethanol tolerance and production phenotypes.

2.5. N-acetylglucosamine biosynthesis

Organisms that do not contain Hfq homologs present an interesting case study for ncRNA pathway engineering strategies. Many of the examples reviewed above that target individual mRNAs for knockdown employ antisense RNA sequences that are stabilized by an Hfq-binding scaffold sequence (Table 1). One alternative for organisms that lack Hfq are PTasRNAs, which utilize base-pairing 5′ and 3′ termini to stabilize a typically longer, target-specific antisense sequence (> 50 nucleotides) (Fig. 1A). However, shorter antisense RNA sequences, like those used in asRNAs with Hfq-binding scaffolds, have been observed to knock down target expression just as effectively as longer sequences (Hoynes-O'Connor and Moon, 2016) and likely limit off-target effects. Thus a second alternative is to heterologously express the Hfq protein alongside the asRNA that contains an Hfq-binding scaffold sequence.

The second strategy has been used to engineer proof-of-concept malonyl-CoA production in the cyanobacterium *Synechocystis* (Sun et al., 2018) (Table 1) and N-acetylglucosamine (GlcNAc) biosynthesis in *Bacillus subtilis*. GlcNAc is a modified form of glucose that is useful as a pharmaceutical to treat osteoarthritis and as dietary supplement to support cartilage health in joints (Chen et al., 2010; Liu et al., 2014b). Because industrial supplies of GlcNAc are primarily obtained through chemical breakdown of chitin from harvested shellfish, more sustainable alternatives are desirable (Table 2) (Chen et al., 2010; Liu et al., 2014b; Sashiwa et al., 2001). *B. subtilis* is an apt host for this pathway because it is generally regarded as a safe industrial organism (Liu et al., 2013a), it is phage-resistant (unlike *E. coli*) (Liu et al., 2013a), and allows for straightforward isolation of the GlcNAc product (Liu et al., 2014b).

GlcNAc can be produced in *B. subtilis* by overexpression of the native *glmS* gene and heterologous overexpression of a single gene, GNA1, from *S. cerevisiae* (Liu et al., 2013b). In this pathway, *glmS* mediates conversion of fructose 6-phosphate to glucosamine-6-phosphate, which is then acetylated by the exogenous GNA1 gene from *S. cerevisiae*. Lastly, n-acetylglucosamine-6-phosphate is dephosphorylated to n-acetylglucosamine (GlcNAc) as it is exported from the cell (Fig. 3D). Importantly, the GlcNAc pathway in *B. subtilis* competes with glycolysis in central carbon metabolism for consumption of fructose-6-phosphate. Additionally, it competes with peptidoglycan synthesis for stores of glucosamine-6-phosphate. The first enzymatic steps of these competing reactions are catalyzed by *pfk* and *glmM*, respectively (Fig. 3D) (Liu et al., 2014b).

Liu et al. specifically selected *pfk* and *glmM* for asRNA knockdown in efforts to minimize consumption of GlcNAc pathway intermediates to competing pathways. An RNA segment antisense to the first 24 nucleotides of each target mRNA's coding sequence (including the start codon) was placed upstream of the MicC Hfq-binding scaffold sequence from *E. coli* followed by a strong terminator. Target enzyme activities were knocked down 60–70% by the asRNAs when Hfq was overexpressed with the asRNAs (relative to strain without asRNAs or Hfq), but only 40% when Hfq was not overexpressed alongside the asRNAs (relative to strain without asRNAs). This difference was used to easily sample two levels of knockdown efficiency for each target. The authors also deleted enzymes responsible for the reverse reactions of the GlcNAc pathway (*gamA*, *nagA,* and *nagB)* and GlcNAc import (*nagP* and *gamP*), as in a previous study (Liu et al., 2013b). Additionally, flux into downstream competing pathways was limited by deleting *ldh* and *pta*, which are responsible for lactate and acetate production, respectively. Coupled with overexpression of the pathway enzymes *glmS* and *GNA1*, overexpression of the anti-*pfk* sRNA, anti-*glmM* sRNA, and *hfq* in the Δ*nagP*, Δ*gamP*, Δ*gamA*, Δ*nagA*, Δ*nagB*, Δ*ldh*, Δ*pta* strain provided for maximum GlcNAc titer, 8.3 g/L. This represents a 2.3-fold increase in titer from the same strain lacking the anti-*pfk* and anti-*glmM* sRNAs and *hfq*. When scaled up to high cell density fed batch fermentation, 31.7 g/L of GlcNAc was obtained (Liu et al., 2014b) (Table 1). Applied together, these asRNA-knockdown and genomic deletion strategies successfully minimized (i) flux through the reverse pathway, (ii) competing consumption of intermediates (both direct and downstream), and (iii) product reimport into the cell. Combined with overexpression of pathway enzymes, these strategies form a basis for development of a more sustainable alternative for the GlcNAc industry.

2.6. Pathways in non-model organisms

As mentioned earlier, organisms that present natural biotechnologically-relevant traits are important systems to study and engineer. Here, we discuss ncRNA engineering strategies applied to *Klebsiella pneumoniae* and *Streptomyces peucetius*, two relatively niche organisms known for their metabolism of glycerol and polyketide pathways, respectively. The ncRNA engineering strategies applied in these organisms represent key initial steps in expanding ncRNA pathway engineering approaches beyond *E. coli*, *C. glutamicum*, and *Clostridium* species.

2.6.1. Biosynthesis of diols and related acids in Klebsiella pneumoniae

Klebsiella pneumoniae, like *C. pasteurianum*, has received attention for its ability to grow on glycerol (Yang et al., 2012; Yazdani and Gonzalez, 2007). It is worth noting that the 1-butanol pathway from *C. acetobutylicum* has been imported into *K. pneumoniae* for this reason. Long asRNAs have been applied to reroute native *K. pneumoniae* glycerol metabolism from 1,3-propanediol and 2,3-butanediol to downstream production of exogenous 1-butanol (Wang et al., 2014) (Fig. 3B). However, improvement to the biosynthesis of native 1,3-propanediol (1,3-PDO) and 2,3-butanediol (2,3-BDO) compounds is also desired. 1,3-PDO is valuable as a precursor to compounds like polytrimethylene terephthalate, a useful polyester in textile manufacturing (Bozell and Petersen, 2010; Kurian, 2005). Derivatives of 2,3-BDO are useful as jet fuel additives and as precursors in rubber, antifreeze, and plastic syntheses (Syu, 2001). 1,3-PDO is typically more valuable and the two compounds are difficult to separate downstream by traditional chemical means (Xiu and Zeng, 2008). As such, pathway engineering strategies have been applied to enrich glycerol consumption in *K. pneumoniae* for 1,3-PDO over 2,3-BDO production. 1,3-PDO is synthesized from glycerol by two reductive steps catalyzed by (1) glycerol dehydratase (encoded by *dhaB1, dhaB2, dhaB3*, *gdrf1,* and *gdrf2*) and (2) 1,3-propanediol oxidoreductase (encoded by *dhaT*) (Fig. 3B). Alternatively, glycerol is processed to pyruvate and is subsequently converted to 2,3-BDO by *budA* (converts pyruvate to α-acetolactate), *budB* (α-acetolactate to acetoin) and *budC* (acetoin to 2,3-BDO) (Fig. 3B).

asRNA-mediated knockdowns of the *budA*, *budB*, and *budC* genes were attempted to redistribute flux across *K. pneumoniae* glycerol processing to minimize 2,3-BDO and maximize 1,3-PDO production (Fig. 3B) (Lu et al., 2016a). These knockdown targets were selected based on (i) the improvement that a prior *budC* deletion imparted to 1,3-PDO biosynthesis (10% increase in 1,3-PDO titer to 22 g/L and 35% decrease in 2,3-BDO titer to 3.4 g/L after 36 h batch culture) (Guo et al., 2013) and (ii) the fact that *budA*, *budB* and *budC* are (up)regulated by the BudR transcription factor, which is known to activate 2,3-BDO

production (Lee et al., 2013). Here, knockdowns were achieved with PTasRNAs (Lu et al., 2016a). In this case, 100 nucleotide segments antisense to a region spanning 50 nucleotides upstream to 50 nucleotides downstream of the RBS of each of *budA*, *budB*, and *budC* were used. Testing each PTasRNA individually in *K. pneumoniae* revealed that both the anti-*budA* and anti-*budB* PTasRNAs limited 2,3-BDO production by approximately 40% to 3 g/L (36 h batch culture) compared to the no PTasRNA control, while anti-*budC* had minimal effect. Similarly, the anti-*budA* and anti-*budB* PTasRNAs each increased 1,3-PDO titer by about 10% to 21.5 g/L compared to the no PTasRNA control (Table 1), while the anti-*budC* PTasRNA had minimal effect (Lu et al., 2016a). Thus, asRNA-mediated knockdown of *budA* or *budB,* provided for a slightly greater decrease in 2,3-BDO titer (40%) than the prior genomic deletion of *budC* (35%) (Guo et al., 2013).

Given that anti-*budA*, -*budB*, and -*budC* all decrease target enzyme activity by 60–70% (Lu et al., 2016a), the lack of impact of anti-*budC* on 2,3-BDO titer may offer insight into the broader pathway. Perhaps the upstream steps catalyzed by *budB* and *budA* are rate limiting such that 70% knockdown of *budC* has negligible impact at 36 h of growth. It is also possible that in this case, a higher level of *budC* knockdown, i.e. one that approaches knockout, may be required for this target to impact pathway titer, as observed in the genomic knockout study (Guo et al., 2013). Additionally, combinatorial knockdown of *budC* with *budB* and/or *budA* may prove fruitful in further minimizing 2,3-butanediol production. More broadly, transcriptomics datasets that profile *K. pneumoniae* gene expression levels under 1,3-PDO production stress will likely offer insight into other genes, potentially in more distant pathways, that could be knocked down to improve 1,3-PDO production.

K. pneumoniae has also been engineered to overproduce 3-hydroxypropionic acid (3-HP), a compound useful as a precursor for acrylic acid and malonic acid (Li et al., 2016b) as well as a monomer in biodegradable polymers (Zhou et al., 2011). 3-HP is biosynthesized by reduction of glycerol in a pathway that differs from that of 1,3-PDO by a single step (Fig. 1B). Rather than 3-hydoxyproprionaldehyde being reduced to 1,3-PDO, it is oxidized to form 3-HP (Fig. 3B).

To increase flux towards the 1,3-PDO and 3-HP branch of *K. pneumoniae* glycerol metabolism, asRNA-mediated knockdowns of *ldh* and *poxB* were pursued to limit competing carbon consumption to lactate and acetate, respectively (Fig. 3B) (Li et al., 2016a). Even though the lactate and acetate pathways branch off of central carbon metabolism at pyruvate and acetyl-CoA, respectively, rather than glycerol, their deletion was still expected to alleviate carbon consumption that competes with 3-HP (Fig. 3B). In this instance, a long asRNA containing a 300 nucleotide sequence antisense to the mRNA sequence conserved across the four *ldh* genes of *K. pneumoniae* was constructed by cloning the antisense sequence between a promoter and a synthetic terminator on a plasmid. Similarly, the anti-*poxB* long asRNA contained a 300 nucleotide sequence antisense to the *poxB* mRNA. These constructs were overexpressed with the *aldH* gene of *E. coli*, which can catalyze the conversion of 3-hydorxyproprionaldehyde to 3-HP, in wild type *K. pneumoniae*. 3-HP titer increased 70% to 1.29 g/L, while lactic acid titer decreased 24% to 1.46 g/L relative to a no asRNA control strain (i.e., *K. pneumoniae* with *aldH* overexpression only) after 24 h of growth (in micro-aerobic flask culture). Similarly, acetic acid titer decreased 50% to 0.6 g/L in the same experiment (Table 1) (Li et al., 2016a).

Importantly, the ncRNA strategy, which targeted multiple *ldh* genes and *poxB*, seemingly had greater impact on 1,3-HP titer (70% increase) than a comparable genome-level approach. While acknowledging the impact that growth conditions can have on pathway yield, genomic deletion of *ldh1*, *ldh2*, and *pta* provided a 14% increase in 3-HP titer (Li et al., 2016b), while the long asRNA strategy yielded a 70% increase (Li et al., 2016a). One possible reason for this difference is that the ncRNA-based strategy targeted 4 genes related to lactate production, rather than 2 in the deletion study. Moreover, the knockdown strategy potentially accessed an intermediate expression level of targeted lactate dehydrogenase (*ldh*) and pyruvate dehydrogenase (*poxB*) enzymes, rather than a full knockout, perhaps providing for greater improvements in 3-HP titer.

2.6.2. Doxorubicin production in Streptomyces peucetius

Streptomyces peucetius natively produces a handful of pharmaceutically active compounds, including ε-rhodomycinone, duanorubicin, and doxorubicin. These related polyketides represent an intermediate and two end products, respectively, of the doxorubicin biosynthesis pathway in *S. peucetius* (Fig. 3E) (Malla et al., 2010b). They are used as antitumor drugs in chemotherapy (Malla et al., 2010b; William Lown, 1993). Due to the difficulty of their chemical synthesis (Malla et al., 2010b), pathway engineering has aimed to enrich the native biosynthetic capabilities of *S. peucetius* for these compounds. Multiple genome-level engineering strategies have improved titer to the range of 40 μg to 10 mg/L (in 3–5 days), including overexpression of enzymes that biosynthesize the TDP-L-duanosamine precursor molecules and overexpression of genes that mediate doxorubicin tolerance and export (Lomovskaya et al., 1998; Malla et al., 2010a; Parajuli et al., 2005). However, further increases are desired.

One noteworthy doxorubicin pathway engineering study focused on eliminating native pathway downregulation by asRNA knockdown of the DoxR transcription factor (Chaudhary et al., 2015b). DoxR represses transcription of the *dnrI* gene (Chaudhary et al., 2014), which encodes a transcription factor that activates expression of many doxorubicin and duanorubicin biosynthesis genes (Tang et al., 1996) (genes indicated by orange shading in Fig. 3E). As such, the authors hypothesized that asRNA-mediated knockdown of the *doxR* mRNA would indirectly activate transcription of pathway biosynthesis genes and improve ε-rhodomycinone, duanorubicin, and doxorubicin titer. An RNA segment antisense to the 5′ UTR, RBS, and first 190 nucleotides of the *doxR* coding sequence was selected and placed in between perfectly base-pairing 5′ and 3′ termini to generate a PTasRNA (as shown in Fig. 1A) targeted to repress *doxR* mRNA translation. Expression of the PTasRNA in a wildtype *S. peucetius* background strain revealed that doxorubicin titer increased 5.8-fold, duanorubicin titer increased 3.6-fold, and ε-rhodomycinone titer increased 1.4-fold after 84 h of growth (relative to wildtype *S. peucetius* without the PTasRNAs) (Table 1). Notably, these effects were much reduced after 96 h of growth, suggesting that further optimization of growth conditions could benefit titer. The asRNA strategy could also be combined with the non-ncRNA-based approaches mentioned above to further improve yields. More generally, further characterization of the role the DoxR and DnrI transcription factors play in *S. peucetius* metabolism may identify other pathways that the anti-*doxR* PTasRNA affects. Perhaps activation of all DoxR-repressed genes may not be beneficial to doxorubicin production. This understanding could be used to refine genes targeted in future engineering of the pathway.

2.7. Emergent themes

Single-target ncRNA engineering approaches like asRNAs, riboswitches, and toehold switches have made substantial impacts in improving titers of the pathways discussed in the above subsections. However, the progress made has been incremental. Native sRNA regulators that naturally target multiple mRNAs offer promising future tools particularly for complex production phenotypes that invoke stress responses; however, they have not yet by fully utilized in this capacity. For example, acid stress survival was improved with ArcZ, DsrA, and RprA overexpression. It should be stressed that this example, and all other examples involving naturally occurring ncRNAs discussed above, involve well-studied natively occurring sRNAs in *E.coli* or those that are well-conserved across bacteria (i.e. the 6 S RNA). Importantly, basic knowledge of the sRNAs, their networks, and their cellular effects were already available to guide rational application for pathway engineering. But even in *E. coli*, the networks and effects of many potentially useful sRNAs remain under-characterized (Wang et al., 2016b). Moreover,

Table 3
Major goals and pathway engineering applications of high-throughput sRNA characterization methods.

Major Goal of Characterization Method	Single or Global sRNA Profiling?	Protein Dependent?	HT sRNA Characterization Technique(s)	(Potential) Applications for Engineering Metabolic Pathways
Target Network	Single	No	MAPS, GRIL-Seq	Analysis of targets can reveal pathways likely regulated by the sRNA. Guides rational pathway engineering with the sRNA.
Target Network	Global[a]	Yes	HITS/PAR/UV-CLIP[b]	Crosslink-induced mutations in cDNA synthesis can indicate RNA-protein binding sites. Applied to Hfq, identified Hfq-sRNA binding sites can reveal new Hfq-binding scaffold sequences for asRNA design[c].
Target Network	Global	Yes	RIL-Seq, CLASH	Analysis of sRNA-target pairs can reveal pathways likely regulated by sRNAs. Can indicate sRNAs that co-regulate mRNAs in a pathway to provide combinatorial sRNA engineering opportunities.
Target Network	Global	No	PARIS	Analysis of sRNA-target pairs can reveal pathways likely regulated by sRNAs. Can indicate sRNAs that co-regulate mRNAs in a pathway to provide combinatorial sRNA engineering opportunities.
Function	Single	No	RNAseq of wildtype and sRNA knockout strains	Analysis of differentially expressed genes can reveal pathways potentially impacted by the sRNA. Paired with MAPS, can indicate regulation of bound targets to better guide rational pathway engineering with the sRNA.
Structure and Function	Single	No	iRS3	Indicates functional structures for molecular engineering of an sRNA regulator. Engineering can alter regulation of sRNA target network to impact phenotype.
Structure and Function	Global	No	INTERFACE	Indicates functional regions within sRNAs. Regions could be targeted to modify sRNA activity and impact phenotype.
Structure	Single	No	SHAPE-Seq	Structural information can guide design of novel RNA regulatory parts.
Structure	Single or Global	No	SHAPE-MaP	Structural information can guide design of novel RNA regulatory parts.

[a] Global information is obtained when a global RNA binding protein, like Hfq or ProQ (which facilate sRNA-mRNA binding), is used
[b] Profiling Hfq gives information on sRNAs and mRNAs bound. sRNA-mRNA pairs are not resolved.
[c] UV Crosslink-induced mutations in cDNA synthesis (obtained in PAR and UV-CLIP) can help identify directly bound mRNA targets

many non-model bacteria that are naturally better-suited than *E. coli* for overproduction of valuable pathways either have no confirmed sRNAs or contain a few confirmed sRNAs, but their target networks and regulatory effects are largely unknown. As a result, there is a need for reliable and convenient techniques that profile sRNA structure, function, and target networks that are readily adaptable across bacterial species.

3. Characterization of native sRNAs for metabolic pathway engineering

In this section, we review recent advances in high-throughput sequencing-based methods that profile the (i) target networks, (ii) function, (iii) and structure of sRNA regulators. Table 3 outlines the discussed techniques, their major goals, and how their results can guide rational pathway engineering with the native sRNA regulators studied. It is worth noting that target network, function, and structure of sRNAs are related: knowledge of an sRNA's target mRNAs, when their functions are annotated, strongly indicates the function of the sRNA. Similarly, methods that profile sRNA structure can also reveal regions of an sRNA that contribute to functional target interactions.

3.1. Characterize sRNA target networks

A hallmark technique in discovering sRNA targets is **M**S2 **a**ffinity **p**urification and **s**equencing (MAPS). This approach aims to identify direct binding partners of a user-defined sRNA by labelling it with the MS2 RNA binding domain sequence. Then, shortly after overexpression of the sRNA is induced, cells are lysed and the sRNA and its bound partners are retrieved by affinity purification with the MS2 RNA binding protein for sequencing (Lalaouna et al., 2015). This technique has been applied to identify likely mRNA targets of the RhyB, RybB, CyaR, and RprA sRNAs in *E. coli* (Lalaouna et al., 2015, 2018) and the RsaA sRNA in *Staphylococcus aureus* (Tomasini et al., 2017). From targets, the function of the sRNA regulator can be surmised. For example, the wealth of iron-processing genes bound by the RyhB sRNA in MAPS data contributed to understanding RyhB as an iron sparing response regulator (Lalaouna et al., 2015). Additionally, deep sequencing of total RNA isolated from wild type and sRNA deletion or overexpression strains can reveal broader pathways differentially expressed as a result of the sRNA and support inference of sRNA function (Massé et al., 2005).

Alternatively, **c**ross**l**inking and **i**mmuno**p**recipitation (CLIP)-based methods focus on identifying the RNAs that are bound to a protein of interest. Frequently called HITS-CLIP when the crosslinking and immunoprecipitation is followed by **hi**gh **t**hroughput **s**equencing (HITS) (Gelderman and Contreras, 2013), this approach relies on covalent crosslinking between the protein of interest and bound RNAs to enable co-purification of the protein and RNAs. Crosslinking is accomplished in a number of ways, including formaldehyde and UV light (254 nm) treatment (Darnell, 2010). HITS-CLIP has been used to profile mRNAs and sRNAs bound to Hfq in *E. coli* (Bilusic et al., 2014), Hfq in *Salmonella typhimurium* (Chao et al., 2012), and CsrA in *E. coli* (Sowa et al., 2017). Additionally, when combined with expression of Hfq protein mutants, it has offered insight into sRNA-Hfq binding mechanisms (Zhang et al., 2013).

However, downstream sequencing of crosslinked, purified RNAs has traditionally included substantial levels of noise, i.e. RNAs not truly bound by the protein are sequenced (Ascano et al., 2012). As such, **p**hoto **a**ctivatable **r**ibonucleoside-enhanced **c**rosslinking and **i**mmuno**p**recipitation (PAR-CLIP) was developed. By incorporating photoactivatable ribonucleosides into RNAs as they are transcribed *in vivo*, true RNA-protein crosslinking (upon treatment with 365 nm light) will prompt characteristic mutations in the RNA that appear as single-nucleotide mismatches in sequencing results. In this way direct, targets can be distinguished from noise and precise binding sites identified. However, this technique has mainly been applied to eukaryotic RNA binding proteins (Ascano et al., 2012). Researchers have obtained similar information for bacterial RNA-protein interactions with **u**ltra**v**iolet-CLIP (UV-CLIP). It has been applied such that characteristic mutations result from high-throughput RNA sequencing without addition of photoactivatable ribonucleosides. Upon cDNA synthesis and sequencing, single-nucleotide mismatches in aligned reads (particularly T to C mutations) can indicate specific protein-RNA binding sites. Performed for Hfq in *Salmonella typhimurium*, this technique captured Hfq-mRNA contact points typically upstream (5′) of predicted mRNA-sRNA binding sites and Hfq-sRNA contact points typically downstream (3′) of predicted sRNA-mRNA binding sites (Holmqvist et al., 2016). Such patterns of Hfq-sRNA binding can provide a basis for advanced definition of Hfq-binding scaffold sequences in asRNA design.

While UV-CLIP can provide insight into mRNAs and sRNAs bound by Hfq and their Hfq binding sites, there is insufficient resolution to identify specific sRNA-mRNA regulator-target pairs. To address the technological gap, Melamed et al. developed **R**NA **i**nteraction by **l**igation and **seq**uencing (RIL-seq). This approach uses UV crosslinking to covalently link RNA binding proteins, such as Hfq, with their bound RNA. Following lysis, immunoprecipitation of the protein-RNA complexes, and RNase digestion, the 3′ and 5′ ends of RNAs in close proximity are ligated to form sRNA-mRNA chimeras. High-throughput sequencing then reveals Hfq dependent sRNA-mRNA regulator-target interactions. Applied in *E. coli,* this approach revealed global changes in Hfq-dependent sRNA-mRNA interactions between exponential phase, stationary phase, and iron-deprived growth conditions. At a single-regulator level, it identified new likely targets for many sRNAs like ArrS, GadY, and GadF (Melamed et al., 2016). For well-characterized and annotated bacteria like *E. coli*, identified targets provide insight in to the pathways the sRNA regulates and the potential phenotypes sRNA overexpression could support. In this way, the RIL-seq study identifies sRNA candidates for pathway engineering.

An analogous method, CLASH (UV-**c**rosslinking, **l**igation, **a**nd **s**equencing of **h**ybrids), was first demonstrated in yeast but has since been adapted for bacteria. This method differs slightly from RIL-Seq in that CLASH ligates RNA linkers to the protein-bound RNAs such that when an sRNA-mRNA complex is bound by a protein, the two RNAs are also ligated together. Applying CLASH to the RNase E protein (*rne*) in pathogenic *E. coli* revealed new targets of multiple sRNAs, including the under-characterized Esr41 sRNA. Notably, identified targets of Esr41 were enriched for iron uptake genes. Follow-up assays confirmed regulatory interaction of Esr41 with *cirA*, *bfr*, and *chuA* (repression), suggesting that Esr41 may play a role in iron stress response. Indeed, deletion of Esr41, provided an advantage in iron limiting conditions (Waters et al., 2017).

Similar to RIL-Seq and CLASH, the GRIL-Seq (**g**lobal small nc**R**NA target **i**dentification by **l**igation and **seq**uencing) method relies on mRNA-sRNA ligation and high-throughput sequencing of resulting chimeras to identify sRNA-mRNA regulator-target pairs. Unlike RIL-seq, which probes the mRNA interactions of many sRNAs expressed natively, GRIL-seq uses a plasmid system to overexpress of an sRNA of interest and a T4 RNA ligase. Post sRNA induction, sRNA-mRNA pairs are ligated *in vivo* upon inducing T4 ligase expression. The chimeric sRNA-mRNA sequences are then recovered by sRNA-specific oligo-functionalized magnetic beads. This approach provides for a greater sequencing depth of a single sRNA's mRNA interactions. Applying GRIL-Seq to the iron stress response PrrF1 sRNA in *Pseudomonas aeruginosa* provided a list of 40 mRNAs most ligated with PrrF1: 36 of 40 correspond to iron processing functions and 17 of 40 are differentially expressed (repressed) due to PrrF1 overexpression, suggesting direct repression by PrrF1 (Han et al., 2016). Perhaps overexpression of PrrF1 would support *Pseudomonas aeruginosa* survival in iron limiting conditions.

The PARIS (**p**soralen **a**nalysis of **R**NA **i**nteraction and **s**tructures) method, showcased in eukaryotic systems, offers insight for how

specific mRNA-sRNA binding pairs could be identified independent of a protein (CLASH, RIL-Seq) and independent of plasmid-based overexpression (GRIL-Seq) in bacteria. PARIS relies on a 4′-aminomehtyltirxsalen psoralen-derivative compound to intercalate RNA helices *in vivo*. When photo-activated (UV 365 nm light treated), the compound covalently crosslinks U residues in the helices. Crosslinked RNA segments are then purified by RNA extraction, partial digestion, and 2D gel purification. Proximity ligation followed by de-crosslinking and sequencing reveals bound RNA segments. This technique has been applied to identify a new snoRNA-rRNA interaction in eukaryotic cells; it also revealed long-range intramolecular RNA-RNA interactions in the XIST long ncRNA, which support and expand current understanding of this molecule's function. This approach holds promise for application in prokaryotes to identify sRNA-mRNA interaction independent of an RNA binding protein (Lu et al., 2016b).

3.2. Discern sRNA structural features

Traditional biochemical techniques that probe RNA structure have also been adapted for *in vivo* high-throughput use (reviewed in (Strobel et al., 2018)). One key method is in-cell SHAPE-Seq (**s**elective 2′-**h**ydroxyl **a**cylation analyzed by **p**rimer **e**xtension and **seq**uencing). SHAPE chemistry has long been applied to interrogate structural accessibility of RNAs (Silverman et al., 2016). In-cell SHAPE-seq involves treating cell cultures endogenously expressing RNAs or overexpressing an RNA of interest with a SHAPE reagent, such as 1-methyl-7-nitroisatoic anhydride (1M7). This compound modifies unstructured, i.e. non-base-paired or accessible, RNA nucleotides such that upon extraction, reverse transcription stalls at the modified nucleotides. cDNA synthesis and sequencing thus reveal a reactivity profile for highly-expressed RNAs in which few reads end at structured nucleotides and many reads end at unstructured nucleotides (Loughrey et al., 2014; Watters et al., 2015). This has been applied to discern common structural features of existing transcriptional attenuators and to define a set of design rules for synthetic transcriptional attenuators. With these rules, 2 new attenuators were designed *in silico* that provided for approximately 80% repression of target gene expression in *E. coli in vivo* (Takahashi et al., 2016).

As illustrated with the *in silico* transcriptional attenuator design, accessibility profiling provides valuable information for engineering RNA molecules. Importantly, it holds promise for expanding beyond overexpression strategies in engineering pathways with sRNAs. One study used an accessibility profile of the CsrB sRNA (obtained from the overexpressed sRNA with the ***in vivo* R**NA **s**tructural **s**ensing **s**ystem, iRS^3 (Sowa et al., 2015; Vazquez et al., 2017)) to infer which of the sRNA's 18 predicted stem-loop structures contributed most and least to functional interactions with its target. In this case, the CsrB sRNA functions by binding many copies of CsrA, a global RNA binding protein regulator. Taking low accessibility to indicate a high contribution to CsrA binding activity (i.e., occlusion by bound CsrA), a small library of 21 variant CsrB sequences was built by rationally redesigning the sRNA with its own modular stem-loop structures. Within the CsrB sRNA, stem-loops that were found to be occluded (low accessibility) were replaced with ones found to be exposed (high accessibility) and *vice versa* to achieve variants representing a range of activity. In total, a nearly 5-fold range in regulator effect was obtained for CsrB and differential impact on glutamate accumulation was observed amongst the variants (Leistra et al., 2017), a known phenotypic effect of CsrB overexpression (McKee et al., 2012).

Given the utility of accessibility-informed ncRNA and sRNA regulator (re)design (Leistra et al., 2017; Takahashi et al., 2016), high-throughput methods that profile the accessibility of all sRNAs simultaneously under their native expression conditions are desirable. One method, SHAPE-MaP (**s**elective 2′-**h**ydroxyl **a**cylation analyzed by **p**rimer **e**xtension and **m**utationa**l** **p**rofiling), has been applied transcriptome-wide in *E. coli* (Mustoe et al., 2018). Very similar to in-cell SHAPE-seq, described above, SHAPE-MaP involves high-throughput transcriptome sequencing of 1M7-treated cells. Here, reverse transcriptases incorporate an incorrect nucleotide at a modified nucleotide to produce a mutation, rather than truncate transcription (Siegfried et al., 2014). Structural profiles curated from accessibility data for ~400 RNAs (mostly mRNAs) were used to recover known and discover new regulatory motifs (Mustoe et al., 2018). Unfortunately, sufficient signal was obtained for only two sRNAs. Pending improvements in sensitivity for sRNAs, high-throughput *in vivo* accessibility profiling may provide unprecedented understanding of sRNA structure and function. Along these lines, the INTERFACE method (***in vivo* t**ranscriptional **e**longation analyzed by **R**NA-seq for **f**unctional **a**ccessibility **c**haracterization in a single **e**xperiment) has been developed to prolife accessibility of multiple sRNAs simultaneously. This technique differs from SHAPE-based methods in that short, antisense oligonucleotides (9–16 base pairs) are used to probe accessibility of specific regions of target RNAs. Importantly, INTERFACE has been used to obtain information about the most likely functional sites of sRNAs *in vivo*, which can guide future rational engineering of sRNA regulators for tunable pathway control (Mihailovic et al., 2018)

4. Challenges of applying ncRNA pathway engineering at the industrial scale

It is important to acknowledge that the majority of the ncRNA pathway engineering examples discussed express the ncRNA on a plasmid (Table 1). As plasmid-based expression is not suitable for scale-up to industrial level fermentation conditions (due to high costs of antibiotic selection), genomic integration of an effective ncRNA is necessary (Lee and Kim, 2015). For example, once plasmid-based expression of the long anti-*pta* sRNA in *C. cellulyticum* was shown to improve ethanol titer, the asRNA was incorporated within the genome. Importantly, impact on ethanol titer was maintained when the asRNA was expressed with a constitutive promoter of similar strength to that of the plasmid-based system (Xu et al., 2017). Although expression of a synthetic asRNA from the *E. coli* genome was not discussed in Section 2, several of the reviewed studies utilized strong constitutive genomic promoters to overexpress non-ncRNA genes of interest in combination with the synthetic asRNA (Na et al., 2013; Noh et al., 2017; Qian et al., 2009, 2011). These tools could be used for genome-level overexpression of the asRNAs as well.

A more general concern in scaling up microbial production schemes is that of phenotype stability across growth conditions and fermentation scales (Lee and Kim, 2015). While many smaller-scale pathway engineering studies quantify titer in shake flask or larger batch cultures, high-volume fed batch fermentation is routinely used in industrial applications (Lee and Kim, 2015). Importantly, some of the examples reviewed in Section 2 demonstrated impact of their ncRNA engineering strategy on product titer in laboratory-scale fed batch fermentations (Liu et al., 2014b; Na et al., 2013; Noh et al., 2017). While these experiments still used plasmid-based expression of the asRNA in fed-batch cultures, they represent important preliminary steps in closing the gap between academic and industrial strain development with ncRNA pathway engineering approaches.

In other examples, the effectiveness of the ncRNA engineering strategy was observed to vary with culture duration (Table 1) (Chaudhary et al., 2015b; Wu et al., 2014; Yang et al., 2015). Given that feedstock composition, culture oxygenation and pH levels, and culture duration all typically vary in scale-up (Lee and Kim, 2015), robustness of ncRNA engineering strategies at the industrial scale is a concern. Particularly, stability of the RNA over longer time scales is a current question. While Hfq binding scaffold sequences and paired-termini have been shown to stabilize asRNAs in small-scale culture (Man et al., 2011; Nakashima et al., 2006), profiling of synthetic asRNA or native sRNA overexpression levels across longer time scales in laboratory-scale fed-batch fermentation is necessary. Further work is needed in this area to

advance ncRNA-based pathway engineering approaches towards the industrial scale. It is important to note that extensive profiling of strains in pilot-scale fed-batch fermentations and iterative strain modifications are typically required, regardless of the pathway engineering strategies employed. Moreover, scale-up of both ncRNA and traditional pathway engineering strategies will benefit from improved metabolic models and integration of omics data (Lee and Kim, 2015).

5. Future outlook and conclusions

ncRNA-based approaches have made substantial impacts in pathway engineering. The relative ease of transfer between strains, applicability to essential genes, and tunability (by varying the asRNA expression level, interaction energy, or location of asRNA binding within a target mRNA), have made asRNA-mediated knockdown a critical tool for metabolic engineers. Space for further pathway optimization may lie in more robust sampling of different designs of the target-specific antisense region of an asRNA. Recent characterization of nearly 100 asRNAs demonstrates several correlations between the target-specific antisense region design and target mRNA knockdown level that should guide future fine-tuning of asRNAs in metabolic pathways (Hoynes-O'Connor and Moon, 2016). Additionally, native sRNA regulators provide powerful handles for eliciting coordinated impact on multiple targets to affect a desired phenotype. Methods are available to identify sRNA-mRNA networks at a high-throughput level. For well-annotated organisms, knowledge of a regulator's targets unlocks their potential phenotypic impact. Coupled with accessibility profiling and molecular information about target interactions, sRNAs can thus be rationally redesigned and engineered beyond overexpression to control cellular phenotypes in a tunable manner. Additionally, synthesizing molecular profiling of sRNA regulators with targetome data may continue to expand the frontier of applying ncRNAs for pathway engineering. Ultimately, success of ncRNA-based pathway engineering methods will require expression profiling of the ncRNA in small-scale fed-batch fermentations, iterative design cycles, and replication of pathway impact at the industrial scale.

Funding

This work was supported by the NSF (Grant nos. MCB-1716777 to L.M.C. and DGE-1610403 to A.N.L.) and the Welch Foundation (Grant no. F-1756 to L.M.C.) for funding.

Competing interests

The authors, A.N.L., N.C.C., and L.M.C., declare no competing interests.

References

Alper, H., Stephanopoulos, G., 2007. Global transcription machinery engineering: a new approach for improving cellular phenotype. Metab. Eng. 9, 258–267.
Altuvia, S., Wagner, E.G.H., 2000. Switching on and off with RNA. Proc. Natl. Acad. Sci. USA 97, 9824.
Ascano, M., Hafner, M., Cekan, P., Gerstberger, S., Tuschl, T., 2012. Identification of RNA–protein interaction networks using PAR-CLIP. Wiley Interdiscip. Rev.: RNA 3, 159–177.
Baseggio, N., Davies, W.D., Davidson, B.E., 1990. Identification of the promoter, operator, and 5′ and 3′ ends of the mRNA of the Escherichia coli K-12 gene aroG. J. Bacteriol. 172, 2547–2557.
Battesti, A., Majdalani, N., Gottesman, S., 2011. The RpoS-mediated general stress response in Escherichia coli. Annu. Rev. Microbiol. 65, 189–213.
Benjamin, C., Ioannis, T., Alexander, L.R., Martin, K.P., 2014. Succinic acid production derived from carbohydrates: an energy and greenhouse gas assessment of a platform chemical toward a bio-based economy. Biofuels, Bioprod. Bioref. 8, 16–29.
Bikard, D., Jiang, W., Samai, P., Hochschild, A., Zhang, F., Marraffini, L.A., 2013. Programmable repression and activation of bacterial gene expression using an engineered CRISPR-Cas system. Nucleic Acids Res. 41, 7429–7437.
Billig, E., 2001. Butyl Alcohols. Kirk-Othmer Encyclopedia of Chemical Technology.
Billig, E., 2003. Butyraldehydes. Kirk-Othmer Encyclopedia of Chemical Technology.
Bilusic, I., Popitsch, N., Rescheneder, P., Schroeder, R., Lybecker, M., 2014. Revisiting the coding potential of the E. coli genome through Hfq co-immunoprecipitation. RNA Biol. 11, 641–654.
Boghigian Brett, A., Zhang, H., Pfeifer Blaine, A., 2011. Multi-factorial engineering of heterologous polyketide production in Escherichia coli reveals complex pathway interactions. Biotechnol. Bioeng. 108, 1360–1371.
Bozell, J.J., Petersen, G.R., 2010. Technology development for the production of biobased products from biorefinery carbohydrates-the US Department of Energy's "Top 10" revisited. Green. Chem. 12, 539–554.
Bozell, J.J., Moens, L., Elliott, D.C., Wang, Y., Neuenscwander, G.G., Fitzpatrick, S.W., Bilski, R.J., Jarnefeld, J.L., 2000. Production of levulinic acid and use as a platform chemical for derived products. Resour. Conserv. Recycl. 28, 227–239.
Bruno, V., 1956. Separation of tyrosine. United States, Patent No. US2738366A.
Calamur, N., Carrera, M., 2005. Propylene. Kirk-Othmer Encyclopedia of Chemical Technology.
Cardinal, E.V., 1953. Separation of tyrosine and cystine. United States, Patent No. US2650242A.
Caron, M.-P., Bastet, L., Lussier, A., Simoneau-Roy, M., Massé, E., Lafontaine, D.A., 2012. Dual-acting riboswitch control of translation initiation and mRNA decay. Proc. Natl. Acad. Sci. USA 109, E3444.
Cavanagh, A.T., Sperger, J.M., Wassarman, K.M., 2012. Regulation of 6S RNA by pRNA synthesis is required for efficient recovery from stationary phase in E. coli and B. subtilis. Nucleic Acids Res. 40, 2234–2246.
Cervin, M.A., Chotani, G.K., Feher, F.J., La Duca, R., McAuliffe, J.C., Miasnikov, A., Peres, C.M., Puhala, A.S., Sanford, K.J., Valle, F., Whited, G.M., 2016. Compositions and methods for producing isoprene. United states, Patent No. US9260727B2.
Chae, T.U., Kim, W.J., Choi, S., Park, S.J., Lee, S.Y., 2015. Metabolic engineering of Escherichia coli for the production of 1,3-diaminopropane, a three carbon diamine. Sci. Rep. 5, 13040.
Chao, Y., Papenfort, K., Reinhardt, R., Sharma, C.M., Vogel, J., 2012. An atlas of Hfq-bound transcripts reveals 3′ UTRs as a genomic reservoir of regulatory small RNAs. EMBO J. 31, 4005–4019.
Chaudhary, A.K., Singh, B., Maharjan, S., Jha, A.K., Kim, B.G., Sohng, J.K., 2014. Switching antibiotics production on and off in actinomycetes by an IclR family transcriptional regulator from Streptomyces peucetius ATCC 27952. J. Microbiol. Biotechnol. 24, 1065–1072.
Chaudhary, A.K., Na, D., Lee, E.Y., 2015a. Rapid and high-throughput construction of microbial cell-factories with regulatory noncoding RNAs. Biotechnol. Adv. 33, 914–930.
Chaudhary, A.K., Pokhrel, A.R., Hue, N.T., Yoo, J.C., Sohng, J.K., 2015b. Paired-termini antisense RNA mediated inhibition of DoxR in Streptomyces peucetius ATCC 27952. Biotechnol. Bioproc. E. 20, 381–388.
Chen, J.-K., Shen, C.-R., Liu, C.-L., 2010. N-Acetylglucosamine: production and applications. Mar. Drugs 8, 2493–2516.
Chen, Y., Indurthi, D.C., Jones, S.W., Papoutsakis, E.T., 2011a. Small RNAs in the genus Clostridium. mBio 2, e00340.
Chen, Z., Meyer, W., Rappert, S., Sun, J., Zeng, A.-P., 2011b. Coevolutionary analysis enabled rational deregulation of allosteric enzyme inhibition in Corynebacterium glutamicum for lysine production. Appl. Environ. Microbiol. 77, 4352–4360.
Chen, Z., Bommareddy, R.R., Frank, D., Rappert, S., Zeng, A.-P., 2014. Deregulation of feedback inhibition of phosphoenolpyruvate carboxylase for improved lysine production in Corynebacterium glutamicum. Appl. Environ. Microbiol. 80, 1388–1393.
Chen, Z., Rappert, S., Zeng, A.-P., 2015. Rational design of allosteric regulation of homoserine dehydrogenase by a nonnatural inhibitor L-lysine. ACS Synth. Biol. 4, 126–131.
Cho, S.H., Lei, R., Henninger, T.D., Contreras, L.M., 2014. Discovery of ethanol responsive small RNAs in Zymomonas mobilis. Appl. Environ. Microbiol. 80, 4189–4198.
Cho, S.H., Haning, K., Contreras, L.M., 2015. Strain engineering via regulatory noncoding RNAs: not a one-blueprint-fits-all. Curr. Opin. Chem. Eng. 10, 25–34.
Choi, K.R., Lee, S.Y., 2016. CRISPR technologies for bacterial systems: current achievements and future directions. Biotechnol. Adv. 34, 1180–1209.
Cobbett, C.S., 1988. Repression of the aroF promoter by the TyrR repressor in Escherichia coli K-12: role of the 'upstream' operator site. Mol. Microbiol. 2, 377–383.
Dakka, J.M., Buchanan, J.S., Chen, J.C., Chen, T., DeCaul, L.C., Helton, T.E., Stanat, J.E., Benitez, F.M., 2012. Process for Producing Phenol and/or Cyclohexanone. United States, Patent No. US8247627B2.
Darnell, R.B., 2010. HITS-CLIP: panoramic views of protein-RNA regulation in living cells. Wiley interdisciplinary reviews. RNA 1, 266–286.
Dasu, V.V., Nakada, Y., Ohnishi-Kameyama, M., Kimura, K., Itoh, Y., 2006. Characterization and a role of Pseudomonas aeruginosa spermidine dehydrogenase in polyamine catabolism. Microbiology 152, 2265–2272.
Davis, M.S., Solbiati, J., Cronan, J.E., 2000. Overproduction of Acetyl-CoA carboxylase activity increases the rate of fatty acid biosynthesis in Escherichia coli. J. Biol. Chem. 275, 28593–28598.
Desvaux, M., 2005. Clostridium cellulolyticum: model organism of mesophilic cellulolytic clostridia. FEMS Microbiol. Rev. 29, 741–764.
Dhingra, V., Rao, K.V., Narasu, M.L., 1999. Current status of artemisinin and its derivatives as antimalarial drugs. Life Sci. 66, 279–300.
Doudna, J.A., Charpentier, E., 2014. The new frontier of genome engineering with CRISPR-Cas9. Science 346.
Dragosits, M., Mattanovich, D., 2013. Adaptive laboratory evolution – principles and applications for biotechnology. Microb. Cell Factor. 12, 64.
Eppelmann, K., Nossin, P.M.M., Raeven, L.J.R.M., Wubbolts, M.G., 2013. Biochemical synthesis of 1,4-butanediamine. United States, Patent No. US8497098B2.
Esquerré, T., Bouvier, M., Turlan, C., Carpousis, A.J., Girbal, L., Cocaign-Bousquet, M., 2016. The Csr system regulates genome-wide mRNA stability and transcription and

thus gene expression in Escherichia coli. Sci. Rep. 6, 25057.
Finn, R.D., Coggill, P., Eberhardt, R.Y., Eddy, S.R., Mistry, J., Mitchell, A.L., Potter, S.C., Punta, M., Qureshi, M., Sangrador-Vegas, A., Salazar, G.A., Tate, J., Bateman, A., 2016. The Pfam protein families database: towards a more sustainable future. Nucleic Acids Res. 44, D279–D285.
Foster, J.W., 2004. Escherichia coli acid resistance: tales of an amateur acidophile. Nat. Rev. Microbiol. 2, 898.
Gaffield, W., Lundin, R.E., Gentili, B., Horowitz, R.M., 1975. C-2 stereochemistry of naringin and its relation to taste and biosynthesis in maturing grapefruit. Bioorg. Chem. 4, 259–269.
Gaida, S.M., Al-Hinai, M.A., Indurthi, D.C., Nicolaou, S.A., Papoutsakis, E.T., 2013. Synthetic tolerance: three noncoding small RNAs, DsrA, ArcZ and RprA, acting supra-additively against acid stress. Nucleic Acids Res. 41, 8726–8737.
Gama-Castro, S., Salgado, H., Santos-Zavaleta, A., Ledezma-Tejeida, D., Muñiz-Rascado, L., García-Sotelo, J.S., Alquicira-Hernández, K., Martínez-Flores, I., Pannier, L., Castro-Mondragón, J.A., Medina-Rivera, A., Solano-Lira, H., Bonavides-Martínez, C., Pérez-Rueda, E., Alquicira-Hernández, S., Porrón-Sotelo, L., López-Fuentes, A., Hernández-Koutoucheva, A., Moral-Chávez, V.D., Rinaldi, F., Collado-Vides, J., 2016. RegulonDB version 9.0: high-level integration of gene regulation, coexpression, motif clustering and beyond. Nucleic Acids Res. 44, D133–D143.
Gao, W.-T., Hou, W.-D., Zheng, M.-R., Tang, L.-J., 2010. Clean and convenient one-pot synthesis of 4-hydroxycoumarin and 4-hydroxy-2-quinolinone derivatives. Synth. Commun. 40, 732–738.
Gelderman, G., Contreras, L., 2013. Discovery of posttranscriptional regulatory RNAs using next generation sequencing technologies. In: Alper, H.S. (Ed.), Systems Metabolic Engineering 985. Humana Press, pp. 269–295.
Gilbert, Luke A., Larson, Matthew H., Morsut, L., Liu, Z., Brar, Gloria A., Torres, Sandra E., Stern-Ginossar, N., Brandman, O., Whitehead, Evan H., Doudna, Jennifer A., Lim, Wendell A., Weissman, Jonathan S., Qi, Lei S., 2013. CRISPR-mediated modular RNA-guided regulation of transcription in Eukaryotes. Cell 154, 442–451.
Gottesman, S., Storz, G., 2011. Bacterial small RNA regulators: versatile roles and rapidly evolving variations. Cold Spring Harb. Perspect. Biol. 3.
Grand View Research, 2014. Global Bio-Succinic Acid Market Size Worth USD 992.8 Million By 2020. 〈https://www.grandviewresearch.com/press-release/bio-succinic-acid-market〉 (Accessed 14 May 2018).
Grand View Research, 2017a. Fuel Ethanol Market Analysis By Product (Starch-Based, Sugar-Based, Cellulosic), By Application (Conventional Vehicles, Flexible Fuel Vehicles), By Region, And Segment Forecasts, 2018 - 2025. 〈https://www.grandviewresearch.com/press-release/global-fuel-ethanol-market〉 (Accessed 14 May 2018).
Grand View Research, 2017b. Isoprene Market Analysis By Type (Polymer Grade, Chemical Grade), By Application (Polyisoprene, Styrene-Isoprene Styrene, Isobutylene-Isoprene Rubber), By End-use, And Segment Forecasts, 2018–2025. 〈https://www.grandviewresearch.com/industry-analysis/isoprene-market〉 (Accessed 14 May 2018).
Guo, X., Fang, H., Zhuge, B., Zong, H., Song, J., Zhuge, J., Du, X., 2013. budC knockout in Klebsiella pneumoniae for bioconversion from glycerol to 1,3-propanediol. Biotechnol. Appl. Biochem. 60, 557–563.
Hale, V., Keasling, J.D., Renninger, N., Diagana, T.T., 2007. Microbially derived artemisinin: a biotechnology solution to the global problem of access to affordable antimalarial drugs. Am. J. Trop. Med. Hyg. 77, 198–202.
Han, K., Tjaden, B., Lory, S., 2016. GRIL-seq provides a method for identifying direct targets of bacterial small regulatory RNA by in vivo proximity ligation. Nat. Microbiol. 2, 16239.
Heatwole, V.M., Somerville, R.L., 1992. Synergism between the Trp repressor and Tyr repressor in repression of the aroL promoter of Escherichia coli K-12. J. Bacteriol. 174, 331–335.
Holmqvist, E., Wright, P.R., Li, L., Bischler, T., Barquist, L., Reinhardt, R., Backofen, R., Vogel, J., 2016. Global RNA recognition patterns of post-transcriptional regulators Hfq and CsrA revealed by UV crosslinking in vivo. EMBO J. 991–1011.
Hör, J., Gorski, S.A., Vogel, J., 2018. Bacterial RNA biology on a genome scale. Mol. Cell.
Hoynes-O'Connor, A., Moon, T.S., 2016. Development of design rules for reliable antisense RNA behavior in E. coli. ACS Synth. Biol. 5, 1441–1454.
Hsu, Patrick D., Lander, Eric S., Zhang, F., 2014. Development and applications of CRISPR-Cas9 for genome engineering. Cell 157, 1262–1278.
Hwang, E.I., Kaneko, M., Ohnishi, Y., Horinouchi, S., 2003. Production of plant-specific flavanones by Escherichia coli containing an artificial gene cluster. Appl. Environ. Microbiol. 69, 2699–2706.
Ikai, H., Yamamoto, S., 1994. Cloning and expression in Escherichia coli of the gene encoding a novel L-2,4-diaminobutyrate decarboxylase of Acinetobacter baumannii. FEMS Microbiol. Lett. 124, 225–228.
Ikai, H., Yamamoto, S., 1997. Identification and analysis of a gene encoding L-2,4-diaminobutyrate:2-ketoglutarate 4-aminotransferase involved in the 1,3-diaminopropane production pathway in Acinetobacter baumannii. J. Bacteriol. 179, 5118–5125.
Ikeda, M., 2005. Towards bacterial strains overproducing L-tryptophan and other aromatics by metabolic engineering. Appl. Microbiol. Biotechnol. 69, 615.
Jang, S., Jang, S., Yang, J., Seo, S.W., Jung, G.Y., 2018. RNA-based dynamic genetic controllers: development strategies and applications. Curr. Opin. Biotechnol. 53, 1–11.
Jones, A.J., Venkataramanan, K.P., Papoutsakis, T., 2016. Overexpression of two stress-responsive, small, non-coding RNAs, 6S and tmRNA, imparts butanol tolerance in Clostridium acetobutylicum. FEMS Microbiol. Lett. 363, fnw063.
Jones, A.J., Fast, A.G., Clupper, M., Papoutsakis, E.T., 2018. Small, low, but potent: the complex regulatory role of the small RNA SolB on solventogenesis in Clostridium acetobutylicum. Appl. Environ. Microbiol.
Juminaga, D., Baidoo, E.E.K., Redding-Johanson, A.M., Batth, T.S., Burd, H., Mukhopadhyay, A., Petzold, C.J., Keasling, J.D., 2012. Modular engineering of L-Tyrosine production in Escherichia coli. Appl. Environ. Microbiol. 78, 89–98.
Kang, Z., Geng, Y., Xia, Y.Z., Kang, J., Qi, Q., 2009. Engineering Escherichia coli for an efficient aerobic fermentation platform. J. Biotechnol. 144, 58–63.
Kang, Z., Wang, Y., Gu, P., Wang, Q., Qi, Q., 2011. Engineering Escherichia coli for efficient production of 5-aminolevulinic acid from glucose. Metab. Eng. 13, 492–498.
Kang, Z., Wang, X., Li, Y., Wang, Q., Qi, Q., 2012. Small RNA RyhB as a potential tool used for metabolic engineering in Escherichia coli. Biotechnol. Lett. 34, 527–531.
Kang, Z., Zhang, C., Zhang, J., Jin, P., Zhang, J., Du, G., Chen, J., 2014. Small RNA regulators in bacteria: powerful tools for metabolic engineering and synthetic biology. Appl. Microbiol. Biotechnol. 98, 3413–3424.
Kang, Z., Zhang, J., Jin, P., Yang, S., 2015. Directed evolution combined with synthetic biology strategies expedite semi-rational engineering of genes and genomes. Bioengineered 6, 136–140.
Kanjee, U., Houry, W.A., 2013. Mechanisms of acid resistance in Escherichia coli. Annu. Rev. Microbiol. 67, 65–81.
Katz, L., Donadio, S., McApline, J., 1998. Recombinant DNA method for producing erythromycin analogs. Patent No. US5824513A.
Kavita, K., de Mets, F., Gottesman, S., 2018. New aspects of RNA-based regulation by Hfq and its partner sRNAs. Curr. Opin. Microbiol. 42, 53–61.
Kazami, J., Mimizuka, T., 2014. Host and Method for Producing Cadaverine. Japan, Patent No. JP5553394B2.
Kim, B., Park, H., Na, D., Lee, S.Y., 2014. Metabolic engineering of Escherichia coli for the production of phenol from glucose. Biotechnol. J. 9, 621–629.
Kind, S., Jeong, W.K., Schröder, H., Wittmann, C., 2010. Systems-wide metabolic pathway engineering in Corynebacterium glutamicum for bio-based production of diaminopentane. Metab. Eng. 12, 341–351.
Konermann, S., Brigham, M.D., Trevino, A.E., Hsu, P.D., Heidenreich, M., Le, C., Platt, R.J., Scott, D.A., Church, G.M., Zhang, F., 2013. Optical control of mammalian endogenous transcription and epigenetic states. Nature 500, 472.
Kreutzer, C., Hans, S., Rieping, M., Mockel, B., Pfeffere, W., Eggeling, L., Sahm, H., Patek, M., 2001. L-lysine-producing corynebacteria and process for the preparation of L-lysine. United States, Patent No. US6200785B1.
Krin, E., Danchin, A., Soutourina, O., 2010. Decrypting the H-NS-dependent regulatory cascade of acid stress resistance in Escherichia coli. BMC Microbiol. 10, 273.
Kumar, V., Ashok, S., Park, S., 2014. Microbial production of 3-hydroxypropionic acid from renewable sources: a green approach as an alternative to conventional chemistry. In: Bisaria, V.S., Kondo, A. (Eds.), Bioprocessing of Renewable Resources to Commodity Bioproducts.
Kurian, J.V., 2005. A new polymer platform for the future — Sorona® from corn derived 1,3-propanediol. J. Polym. Environ. 13, 159–167.
Kushwaha, M., Rostain, W., Prakash, S., Duncan, J.N., Jaramillo, A., 2016. Using RNA as molecular code for programming cellular function. ACS Synth. Biol. 5, 795–809.
Lalaouna, D., Carrier, M.-C., Semsey, S., Brouard, J.-S., Wang, J., Wade, Joseph T., Massé, E., 2015. A 3′ external transcribed spacer in a tRNA transcript acts as a sponge for small RNAs to prevent transcriptional noise. Mol. Cell. 58, 393–405.
Lalaouna, D., Prévost, K., Laliberté, G., Houé, V., Massé, E., 2018. Contrasting silencing mechanisms of the same target mRNA by two regulatory RNAs in Escherichia coli. Nucleic Acids Res. 46, 2600–2612.
Lawley, B., Pittard, A.J., 1994. Regulation of aroL expression by TyrR protein and Trp repressor in Escherichia coli K-12. J. Bacteriol. 176, 6921–6930.
Lease, R.A., Belfort, M., 2000. A trans-acting RNA as a control switch in < em > Escherichia coli < /em > : DsrA modulates function by forming alternative structures. Proc. Natl. Acad. Sci. USA 97, 9919.
Lee, J.W., Na, D., Park, J.M., Lee, J., Choi, S., Lee, S.Y., 2012. Systems metabolic engineering of microorganisms for natural and non-natural chemicals. Nat. Chem. Biol. 8, 536.
Lee, S., Kim, B., Jeong, D., Oh, M., Um, Y., Kim, Y.-R., Kim, J., Lee, J., 2013. Observation of 2,3-butanediol biosynthesis in Lys regulator mutated Klebsiella pneumoniae at gene transcription level. J. Biotechnol. 168, 520–526.
Lee, S.Y., Kim, H.U., 2015. Systems strategies for developing industrial microbial strains. Nat. Biotechnol. 33, 1061.
Lee, Y.J., Moon, T.S., 2018. Design rules of synthetic non-coding RNAs in bacteria. Methods.
Lee Sang, Y., Park Jin, H., Jang Seh, H., Nielsen Lars, K., Kim, J., Jung Kwang, S., 2008. Fermentative butanol production by clostridia. Biotechnol. Bioeng. 101, 209–228.
Leistra, A.N., Amador, P., Buvanendiran, A., Moon-Walker, A., Contreras, L.M., 2017. Rational modular RNA engineering based on In vivo profiling of structural accessibility. ACS Synth. Biol.
Leonard, E., Yan, Y., Fowler, Z.L., Li, Z., Lim, C.-G., Lim, K.-H., Koffas, M.A.G., 2008. Strain improvement of recombinant escherichia coli for efficient production of plant flavonoids. Mol. Pharm. 5, 257–265.
Leuchtenberger, W., Huthmacher, K., Drauz, K., 2005. Biotechnological production of amino acids and derivatives: current status and prospects. Appl. Microbiol. Biotechnol. 69, 1–8.
Li, F., Wang, Y., Gong, K., Wang, Q., Liang, Q., Qi, Q., 2014. Constitutive expression of RyhB regulates the heme biosynthesis pathway and increases the 5-aminolevulinic acid accumulation in Escherichia coli. FEMS Microbiol. Lett. 350, 209–215.
Li, W., Ying, X., Lu, Q., Chen, L., 2012a. Predicting sRNAs and their targets in bacteria. Genom. Proteom. Bioinforma. 10, 276–284.
Li, Y., Tschaplinski, T.J., Engle, N.L., Hamilton, C.Y., Rodriguez, M., Liao, J.C., Schadt, C.W., Guss, A.M., Yang, Y., Graham, D.E., 2012b. Combined inactivation of the Clostridium cellulolyticum lactate and malate dehydrogenase genes substantially increases ethanol yield from cellulose and switchgrass fermentations. Biotechnol. Biofuels 5, 2.
Li, Y., Li, S., Ge, X., Tian, P., 2016a. Development of a Red recombinase system and

antisense RNA technology in Klebsiella pneumoniae for the production of chemicals. RSC Adv. 6, 79920–79927.
Li, Y., Wang, X., Ge, X., Tian, P., 2016b. High production of 3-hydroxypropionic acid in Klebsiella pneumoniae by systematic optimization of glycerol metabolism. Sci. Rep. 6, 26932.
Lim, C.G., Fowler, Z.L., Hueller, T., Schaffer, S., Koffas, M.A.G., 2011. High-yield resveratrol production in engineered Escherichia coli. Appl. Environ. Microbiol. 77, 3451–3460.
Lin, J., Fu, W., Cen, P., 2009. Characterization of 5-aminolevulinate synthase from Agrobacterium radiobacter, screening new inhibitors for 5-aminolevulinate dehydratase from Escherichia coli and their potential use for high 5-aminolevulinate production. Bioresour. Technol. 100, 2293–2297.
Lin, Y., Shen, X., Yuan, Q., Yan, Y., 2013. Microbial biosynthesis of the anticoagulant precursor 4-hydroxycoumarin. Nat. Commun. 4, 2603.
Liu, C.-L., Lv, Q., Tan, T.-W., 2015. Joint antisense RNA strategies for regulating isoprene production in Escherichia coli. RSC Adv. 5, 74892–74898.
Liu, L., Liu, Y., Shin, H.-D., Chen, R., Li, J., Du, G., Chen, J., 2013a. Microbial production of glucosamine and N-acetylglucosamine: advances and perspectives. Appl. Microbiol Biotechnol. 97, 6149–6158.
Liu, M.Y., Gui, G., Wei, B., Preston 3rd, J.F., Oakford, L., Yuksel, U., Giedroc, D.P., Romeo, T., 1997. The RNA molecule CsrB binds to the global regulatory protein CsrA and antagonizes its activity in Escherichia coli. J. Biol. Chem. 272, 17502–17510.
Liu, S., Zhang, G., Li, X., Zhang, J., 2014a. Microbial production and applications of 5-aminolevulinic acid. Appl. Microbiol. Biotechnol. 98, 7349–7357.
Liu, Y., Liu, L., Shin, H.-D., Chen, R.R., Li, J., Du, G., Chen, J., 2013b. Pathway engineering of Bacillus subtilis for microbial production of N-acetylglucosamine. Metab. Eng. 19, 107–115.
Liu, Y., Zhu, Y., Li, J., Shin, H.-D., Chen, R.R., Du, G., Liu, L., Chen, J., 2014b. Modular pathway engineering of Bacillus subtilis for improved N-acetylglucosamine production. Metab. Eng. 23, 42–52.
Logsdon, J.E., 2004. Ethanol. Kirk-Othmer Encyclopedia of Chemical Technology.
Lomovskaya, N., Doi-Katayama, Y., Filippini, S., Nastro, C., Fonstein, L., Gallo, M., Colombo, A.L., Hutchinson, C.R., 1998. The Streptomyces peucetius dpsY and dnrX genes govern early and late steps of daunorubicin and doxorubicin biosynthesis. J. Bacteriol. 180, 2379–2386.
Loughrey, D., Watters, K.E., Settle, A.H., Lucks, J.B., 2014. SHAPE-Seq. 2.0: systematic optimization and extension of high-throughput chemical probing of RNA secondary structure with next generation sequencing. Nucleic Acids Res. 42 (e165-e165).
Lu, X., Ji, G., Zong, H., Zhuge, B., 2016a. The role of budABC on 1,3-propanediol and 2,3-butanediol production from glycerol in Klebsiella pneumoniae CICIM B0057. Bioengineered 7, 439–444.
Lu, Z., Zhang, Qiangfeng, C., Lee, B., Flynn, Ryan, A., Smith, Martin, A., Robinson, James, T., Davidovich, C., Gooding, Anne, R., Goodrich, Karen J., Mattick, John S., Mesirov, Jill P., Cech, Thomas R., Chang, Howard Y., 2016b. RNA duplex map in living cells reveals higher-order transcriptome structure. Cell 165, 1267–1279.
Lütke-Eversloh, T., Bahl, H., 2011. Metabolic engineering of Clostridium acetobutylicum: recent advances to improve butanol production. Curr. Opin. Biotechnol. 22, 634–647.
Lütke-Eversloh, T., Stephanopoulos, G., 2007. L-Tyrosine production by deregulated strains of Escherichia coli. Appl. Microbiol. Biotechnol. 75, 103–110.
Lütke-Eversloh, T., Stephanopoulos, G., 2008. Combinatorial pathway analysis for improved L-tyrosine production in Escherichia coli: identification of enzymatic bottlenecks by systematic gene overexpression. Metab. Eng. 10, 69–77.
Lütke-Eversloh, T., Santos, C.N.S., Stephanopoulos, G., 2007. Perspectives of biotechnological production of L-tyrosine and its applications. Appl. Microbiol. Biotechnol. 77, 751–762.
Lybarger, H.M., 2014. Isoprene. Kirk-Othmer Encyclopedia of Chemical Technology.
Magnuson, K., Jackowski, S., Rock, C.O., Cronan, J.E., 1993. Regulation of fatty acid biosynthesis in Escherichia coli. Microbiol. Rev. 57, 522–542.
Malla, S., Niraula, N.P., Liou, K., Sohng, J.K., 2010a. Self-resistance mechanism in Streptomyces peucetius: overexpression of drrA, drrB and drrC for doxorubicin enhancement. Microbiol. Res. 165, 259–267.
Malla, S., Prasad Niraula, N., Singh, B., Liou, K., Kyung Sohng, J., 2010b. Limitations in doxorubicin production from Streptomyces peucetius. Microbiol. Res. 165, 427–435.
Man, S., Cheng, R., Miao, C., Gong, Q., Gu, Y., Lu, X., Han, F., Yu, W., 2011. Artificial trans -encoded small non-coding RNAs specifically silence the selected gene expression in bacteria. Nucleic Acids Res. 39 (e50-e50).
Marcheschi, R.J., Gronenberg, L.S., Liao, J.C., 2013. Protein engineering for metabolic engineering: current and next-generation tools. Biotechnol. J. 8, 545–555.
Markets and Markets, 2015. 1,3-Propanediol (PDO) Market by Applications (PTT, Polyurethane, Cosmetic, Personal Care & Home Cleaning & Others) & Geography - Global Market Trends & Forecasts to 2021. 〈https://www.marketsandmarkets.com/Market-Reports/1-3-propanediol-pdo-market-760.html〉 (Accessed 14 May 2018).
Markets and Markets, 2017. Food Amino Acids Market by Application (Nutraceutical & Dietary Supplements, Infant Formula, Food Fortification, Convenience Foods), Type (Glutamic Acid, Lysine, Tryptophan, Methionine), Source (Plant, Animal, Synthetic), and Region - Global Forecast to 2022. 〈https://www.marketsandmarkets.com/PressReleases/food-amino-acids.asp〉 (Accessed 14 May 2018).
Markets and Markets, 2018. n-Butanol Market by Application (Butyl Acrylate, Butyl Acetate, Glycol Ethers, Direct Solvents, Plasticizers), and Region (Asia Pacific, North America, Europe, Middle East & Africa, South America) - Global Forecast to 2022. 〈https://www.marketsandmarkets.com/Market-Reports/n-butanol-market-1089.html〉 (Accessed 14 May 2018).
Martin, V.J.J., Pitera, D.J., Withers, S.T., Newman, J.D., Keasling, J.D., 2003. Engineering a mevalonate pathway in Escherichia coli for production of terpenoids. Nat. Biotechnol. 21, 796.
Massé, E., Vanderpool, C.K., Gottesman, S., 2005. Effect of RyhB small RNA on global iron use in Escherichia coli. J. Bacteriol. 187, 6962–6971.
Maurice, M.A., 1939. Isolation of leucine and tyrosine from corn gluten. United States, Patent No. US2178210A.
McKee, A., Rutherford, B., Chivian, D., Baidoo, E., Juminaga, D., Kuo, D., Benke, P., Dietrich, J., Ma, S., Arkin, A., Petzold, C., Adams, P., Keasling, J., Chhabra, S., 2012. Manipulation of the carbon storage regulator system for metabolite remodeling and biofuel production in Escherichia coli. Microb. Cell Fact. 11, 79.
McKinlay, J.B., Vieille, C., Zeikus, J.G., 2007. Prospects for a bio-based succinate industry. Appl. Microbiol. Biotechnol. 76, 727–740.
Melamed, S., Peer, A., Faigenbaum-Romm, R., Gatt, Y.E., Reiss, N., Bar, A., Altuvia, Y., Argaman, L., Margalit, H., 2016. Global mapping of small RNA-target interactions in bacteria. Mol. Cell. 63, 884–897.
Mellin, J.R., Cossart, P., 2015. Unexpected versatility in bacterial riboswitches. Trends Genet. 31, 150–156.
Meng, H.L., Xiong, Z.Q., Song, S.J., Wang, J., Wang, Y., 2015. Construction of polyketide overproducing Escherichia coli strains via synthetic antisense RNAs based on in silico fluxome analysis and comparative transcriptome analysis. Biotechnol. J. 11, 530–541.
Mihailovic, M.K., Vazquez-Anderson, J., Li, Y., Fry, V., Vimalathas, P., Herrera, D., Lease, R.A., Powell, W.B., Contreras, L.M., 2018. High-throughput in vivo mapping of RNA accessible interfaces to identify functional sRNA binding sites. Nat. Commun. 9, 4084.
Mimitsuka, T., Sawai, H., Hatsu, M., Yamada, K., 2007. Metabolic engineering of Corynebacterium glutamicum for Cadaverine Fermentation. Biosci. Biotechnol. Biochem. 71, 2130–2135.
Morin, M., Ropers, D., Letisse, F., Laguerre, S., Portais, J.-C., Cocaign-Bousquet, M., Enjalbert, B., 2016. The post-transcriptional regulatory system CSR controls the balance of metabolic pools in upper glycolysis of Escherichia coli. Mol. Microbiol. 686–700.
Mustoe, A.M., Busan, S., Rice, G.M., Hajdin, C.E., Peterson, B.K., Ruda, V.M., Kubica, N., Nutiu, R., Baryza, J.L., Weeks, K.M., 2018. Pervasive regulatory functions of mRNA structure revealed by high-resolution SHAPE probing. Cell 173, 181–195 (e18).
Na, D., Yoo, S.M., Chung, H., Park, H., Park, J.H., Lee, S.Y., 2013. Metabolic engineering of Escherichia coli using synthetic small regulatory RNAs. Nat. Biotechnol. 31, 170–174.
Nakashima, N., Tamura, T., Good, L., 2006. Paired termini stabilize antisense RNAs and enhance conditional gene silencing in Escherichia coli. Nucleic Acids Res. 34 (e138-e138).
Nielsen, J., Keasling, Jay D.,, 2016. Engineering cellular metabolism. Cell 164, 1185–1197.
Nitzan, M., Rehani, R., Margalit, H., 2017. Integration of bacterial small RNAs in regulatory networks. Annu. Rev. Biophys. 46, 131–148.
Noh, M., Yoo, S.M., Kim, W.J., Lee, S.Y., 2017. Gene expression knockdown by modulating synthetic small RNA expression in Escherichia coli. Cell Syst. 5, 418–426 (e4).
Nonomura, S., Kanagawa, H., Makimoto, A., 1963. Chemical constituents of Polygonaceous plants. I studies on the components of Ko-jô-kon. (Polygonum cuspidatum SIEB. et ZUCC.). Yakugaku Zasshi 83, 988–990.
Ohinata, T., Takayanagi, Y., 2003. Production of 1,3-diaminopropane. Japan, Patent No. JP3417597B2.
Ohnishi, J., Mitsuhashi, S., Hayashi, M., Ando, S., Yokoi, H., Ochiai, K., Ikeda, M., 2002. A novel methodology employing Corynebacterium glutamicum genome information to generate a new L-lysine-producing mutant. Appl. Microbiol. Biotechnol. 58.
Ohnishi, J., Katahira, R., Mitsuhashi, S., Kakita, S., Ikeda, M., 2005. A novel gnd mutation leading to increased L-lysine production in Corynebacterium glutamicum. FEMS Microbiol. Lett. 242, 265–274.
Ooyen, J.V., Noack, S., Bott, M., Reth, A., Eggeling, L., 2012. Improved L-lysine production with Corynebacterium glutamicum and systemic insight into citrate synthase flux and activity. Biotechnol. Bioeng. 109, 2070–2081.
Parajuli, N., Viet, H.T., Ishida, K., Tong, H.T., Lee, H.C., Liou, K., Sohng, J.K., 2005. Identification and characterization of the afsR homologue regulatory gene from Streptomyces peucetius ATCC 27952. Res. Microbiol. 156, 707–712.
Park, H., Yoon, Y., Suk, S., Lee, J.Y., Lee, Y., 2014. Effects of different target sites on antisense RNA-mediated regulation of gene expression. BMB Rep. 47, 619–624.
Peng, Q., Berg, K., Moan, J., Kongshaug, M., Nesland, J.M., 1997. 5-Aminolevulinic acid-based photodynamic therapy: principles and experimental research. Photochem. Photobiol. 65, 235–251.
Persistence Market Research, 2017. Phenol Market to Push Past a Value of US$ 17 Billion by End of 2022; Cumene Manufacturing Process to Hold the Key to Success. 〈https://www.persistencemarketresearch.com/mediarelease/phenol-market.asp〉 (Accessed 14 May 2018).
Pfeifer, B.A., Admiraal, S.J., Gramajo, H., Cane, D.E., Khosla, C., 2001. Biosynthesis of complex polyketides in a metabolically engineered strain of E. coli. Science 291, 1790.
Pittard, J., Camakaris, H., Yang, J., 2005. The TyrR regulon. Mol. Microbiol. 55, 16–26.
Powell, R.G., TePaske, M.R., Plattner, R.D., White, J.F., Clement, S.L., 1994. Isolation of resveratrol from Festuca versuta and evidence for the widespread occurrence of this stilbene in the poaceae. Phytochemistry 35, 335–338.
Pyne, E.M., Moo-Young, M., Chung, A.D., Chou, P.C., 2015. Antisense-RNA-mediated gene downregulation in Clostridium pasteurianum. Fermentation 1.
Qi, L.S., Arkin, A.P., 2014. A versatile framework for microbial engineering using synthetic non-coding RNAs. Nat. Rev. Microbiol. 12, 341.
Qi, Lei S., Larson, Matthew H., Gilbert, Luke A., Doudna, Jennifer A., Weissman, Jonathan S., Arkin, Adam P., Lim, Wendell A.,, 2013. Repurposing CRISPR as an RNA-guided platform for sequence-specific control of gene expression. Cell 152, 1173–1183.
Qian, Z.G., Xia, X.X., Lee Sang, Y., 2009. Metabolic engineering of Escherichia coli for the production of putrescine: a four carbon diamine. Biotechnol. Bioeng. 104, 651–662.

Qian, Z.G., Xia, X.X., Lee, S.Y., 2011. Metabolic engineering of Escherichia coli for the production of cadaverine: a five carbon diamine. Biotechnol. Bioeng. 108, 93–103.
Ro, D.-K., Paradise, E.M., Ouellet, M., Fisher, K.J., Newman, K.L., Ndungu, J.M., Ho, K.A., Eachus, R.A., Ham, T.S., Kirby, J., Chang, M.C.Y., Withers, S.T., Shiba, Y., Sarpong, R., Keasling, J.D., 2006. Production of the antimalarial drug precursor artemisinic acid in engineered yeast. Nature 440, 940.
Rodionov, D.A., Vitreschak, A.G., Mironov, A.A., Gelfand, M.S., 2003. Regulation of lysine biosynthesis and transport genes in bacteria: yet another RNA riboswitch? Nucleic Acids Res. 31, 6748–6757.
Rodrigo, G., Landrain, T.E., Shen, S., Jaramillo, A., 2013. A new frontier in synthetic biology: automated design of small RNA devices in bacteria. Trends Genet. 29, 529–536.
Rodriguez, A., Martnez, J.A., Flores, N., Escalante, A., Gosset, G., Bolivar, F., 2014. Engineering Escherichia coli to overproduce aromatic amino acids and derived compounds. Microb. Cell Factor. 13, 126.
Romeo, T., 1998. Global regulation by the small RNA-binding protein CsrA and the non-coding RNA molecule CsrB. Mol. Microbiol. 29, 1321–1330.
Romeo, T., Vakulskas, C.A., Babitzke, P., 2013. Post-transcriptional regulation on a global scale: form and function of Csr/Rsm systems. Environ. Microbiol. 15, 313–324.
Sanders, J., Scott, E., Weusthuis, R., Mooibroek, H., 2007. Bio-refinery as the bio-inspired process to bulk chemicals. Macromol. Biosci. 7, 105–117.
Santos, C.N.S., Koffas, M., Stephanopoulos, G., 2011. Optimization of a heterologous pathway for the production of flavonoids from glucose. Metab. Eng. 13, 392–400.
Sasaki, K., Watanabe, M., Tanaka, T., Tanaka, T., 2002. Biosynthesis, biotechnological production and applications of 5-aminolevulinic acid. Appl. Microbiol. Biotechnol. 58, 23–29.
Sashiwa, H., Fujishima, S., Yamano, N., Kawasaki, N., Nakayama, A., Muraki, E., Aiba, S.-I., 2001. Production of N-acetyl-D-glucosamine from β-Chitin by enzymatic hydrolysis. Chem. Lett. 30, 308–309.
Schmidt, R.J., 2005. Industrial catalytic processes—phenol production. Appl. Catal. A: General. 280, 89–103.
Schwarz, K.M., Grosse-Honebrink, A., Derecka, K., Rotta, C., Zhang, Y., Minton, N.P., 2017. Towards improved butanol production through targeted genetic modification of Clostridium pasteurianum. Metab. Eng. 40, 124–137.
Sharma, C.M., Vogel, J., 2014. Differential RNA-seq: the approach behind and the biological insight gained. Curr. Opin. Microbiol. 19, 97–105.
Siegfried, N.A., Busan, S., Rice, G.M., Nelson, J.A.E., Weeks, K.M., 2014. RNA motif discovery by SHAPE and mutational profiling (SHAPE-MaP). Nat. Methods 11, 959.
Silverman, I.M., Berkowitz, N.D., Gosai, S.J., Gregory, B.D., 2016. Genome-wide approaches for RNA structure probing. In: Yeo, G.W. (Ed.), RNA Processing: Disease and Genome-wide Probing. Springer International Publishing, Cham, pp. 29–59.
Song, C.W., Lee, J., Lee, S.Y., 2015. Genome engineering and gene expression control for bacterial strain development. Biotechnol. J. 10, 56–68.
Sowa, S.W., Vazquez-Anderson, J., Clark, C.A., De La Peña, R., Dunn, K., Fung, E.K., Khoury, M.J., Contreras, L.M., 2015. Exploiting post-transcriptional regulation to probe RNA structures in vivo via fluorescence. Nucleic Acids Res. 43, e13.
Sowa, S.W., Gelderman, G., Leistra, A.N., Buvanendiran, A., Lipp, S., Pitaktong, A., Vakulskas, C.A., Romeo, T., Baldea, M., Contreras, L.M., 2017. Integrative FourD omics approach profiles the target network of the carbon storage regulatory system. Nucleic Acids Res. 45, 1673–1686.
Stephanopoulos, G., Sinskey, A.J., 1993. Metabolic engineering — methodologies and future prospects. Trends Biotechnol. 11, 392–396.
Storz, G., Vogel, J., Wassarman, Karen M.,, 2011. Regulation by small RNAs in bacteria: expanding frontiers. Mol. Cell. 43, 880–891.
Strobel, E.J., Yu, A.M., Lucks, J.B., 2018. High-throughput determination of RNA structures. Nat. Rev. Genet. 19, 615–634.
Sun, T., Li, S., Song, X., Pei, G., Diao, J., Cui, J., Shi, M., Chen, L., Zhang, W., 2018. Redirection of carbon flux to key precursor malonyl-CoA via artificial small RNAs in photosynthetic Synechocystis sp. PCC 6803. Biotechnol. Biofuels. 11, 26.
Sun, Y., Ma, C., Fu, H., Mu, Y., Xiu, Z., 2014. 1,3-Propanediol. In: Bisaria, V.A., Kondo, A. (Eds.), Bioprocessing of Renewable Resources to Commodity Bioproducts.
Sundaram, K.M., Shreehan, M.M., Olszewski, E.F., 2010. Ethylene. Kirk-Othmer Encyclopedia of Chemical Technology.
Syu, M.-J., 2001. Biological production of 2,3-butanediol. Appl. Microbiol. Biotechnol. 55, 10–18.
Takahashi, M.K., Watters, K.E., Gasper, P.M., Abbott, T.R., Carlson, P.D., Chen, A.A., Lucks, J.B., 2016. Using in-cell shape-seq and simulations to probe structure–function design principles of RNA transcriptional regulators. RNA 920–933.
Takeya, H., Shimizu, T., Ueki, H., 1996. Process for preparing 5-aminolevulinic acid. Patent No. EP0607952B1.
Tang, L., Grimm, A., Zhang, Y.-X., Hutchinson, C.R., 1996. Purification and characterization of the DNA-binding protein DnrI, a transcriptional factor of daunorubicin biosynthesis in Streptomyces peucetius. Mol. Microbiol. 22, 801–813.
Thakker, C., Martínez, I., San, K.Y., Bennett George, N., 2011. Succinate production in Escherichia coli. Biotechnol. J. 7, 213–224.
Tomasini, A., Moreau, K., Chicher, J., Geissmann, T., Vandenesch, F., Romby, P., Marzi, S., Caldelari, I., 2017. The RNA targetome of Staphylococcus aureus non-coding RNA RsaA: impact on cell surface properties and defense mechanisms. Nucleic Acids Res. 45, 6746–6760.
Vakulskas, C.A., Potts, A.H., Babitzke, P., Ahmer, B.M.M., Romeo, T., 2015. Regulation of Bacterial Virulence by Csr (Rsm) Systems. Microbiol. Mol. Biol. Rev. 79, 193–224.
Vakulskas, C.A., Leng, Y., Abe, H., Amaki, T., Okayama, A., Babitzke, P., Suzuki, K., Romeo, T., 2016. Antagonistic control of the turnover pathway for the global regulatory sRNA CsrB by the CsrA and CsrD proteins. Nucleic Acids Res. 44, 7896–7910.
Vazquez, J., Mihailovic, M., Baldridge, K.C., Haning, K., Cho, S.H., Contreras, L.M., 2017. Optimization of a novel biophysical model using large scale in vivo antisense RNA hybridization data in bacteria displays improved prediction capabilities. Nucleic Acids Res. 45, 5523–5538.
Vazquez-Anderson, J., Contreras, L.M., 2013. Regulatory RNAs: charming gene management styles for synthetic biology applications. RNA Biol. 10, 1778–1797.
Venkataramanan, K.P., Jones, S.W., McCormick, K.P., Kunjeti, S.G., Ralston, M.T., Meyers, B.C., Papoutsakis, E.T., 2013. The Clostridium small RNome that responds to stress: the paradigm and importance of toxic metabolite stress in C. acetobutylicum. BMC Genom. 14, 849.
Vickers, C.E., Sabri, S., 2015. Isoprene. In: Schrader, J., Bohlmann, J. (Eds.), Biotechnology of Isoprenoids. Springer International Publishing, Cham, pp. 289–317.
Villa, J.K., Su, Y., Contreras, L.M., Hammond, M.C., 2017. Synthetic biology of small RNAs and riboswitches. Microbiol. Spectr. 6.
Vogel, J., Luisi, B.F., 2011. Hfq and its constellation of RNA. Nat. Rev. Microbiol. 9, 578–589.
Wagner, E.G.H., Romby, P., 2015. Chapter three - small RNAs in Bacteria and Archaea: who they are, what they do, and how they do it. In: Friedmann, T., Dunlap, J.C., Goodwin, S.F. (Eds.), Advances in Genetics 90. Academic Press, pp. 133–208.
Wang, H., La Russa, M., Qi, L.S., 2016a. CRISPR/Cas9 in genome editing and beyond. Annu. Rev. Biochem. 85, 227–264.
Wang, H.H., Isaacs, F.J., Carr, P.A., Sun, Z.Z., Xu, G., Forest, C.R., Church, G.M., 2009. Programming cells by multiplex genome engineering and accelerated evolution. Nature 460, 894–898.
Wang, J., Rennie, W., Liu, C., Carmack, C.S., Prévost, K., Caron, M.-P., Massé, E., Ding, Y., Wade, J.T., 2015. Identification of bacterial sRNA regulatory targets using ribosome profiling. Nucleic Acids Res. 43, 10308–10320.
Wang, J., Liu, T., Zhao, B., Lu, Q., Wang, Z., Cao, Y., Li, W., 2016b. sRNATarBase 3.0: an updated database for sRNA-target interactions in bacteria. Nucleic Acids Res. 44, D248–D253.
Wang, J., Wang, H., Yang, L., Lv, L., Zhang, Z., Ren, B., Dong, L., Li, N., 2018a. A novel riboregulator switch system of gene expression for enhanced microbial production of succinic acid. J. Ind. Microbiol. Biotechnol. 45, 253–269.
Wang, M., Fan, L., Tan, T., 2014. 1-Butanol production from glycerol by engineered Klebsiella pneumoniae. RSC Adv. 4, 57791–57798.
Wang, X., Dubey, A.K., Suzuki, K., Baker, C.S., Babitzke, P., Romeo, T., 2005. CsrA post-transcriptionally represses pgaABCD, responsible for synthesis of a biofilm polysaccharide adhesin of Escherichia coli. Mol. Microbiol. 56, 1648–1663.
Wang, X., He, Q., Yang, Y., Wang, J., Haning, K., Hu, Y., Wu, B., He, M., Zhang, Y., Bao, J., Contreras, L.M., Yang, S., 2018b. Advances and prospects in metabolic engineering of Zymomonas mobilis. Metab. Eng.
Waters, S.A., McAteer, S.P., Kudla, G., Pang, I., Deshpande, N.P., Amos, T.G., Leong, K.W., Wilkins, M.R., Strugnell, R., Gally, D.L., Tollervey, D., Tree, J.J., 2017. Small RNA interactome of pathogenic E. coli revealed through crosslinking of RNase E. EMBO J. 36, 374–387.
Watters, K.E., Abbott, T.R., Lucks, J.B., 2015. Simultaneous characterization of cellular RNA structure and function with in-cell SHAPE-Seq. Nucleic Acids Res. 44, e12.
Wendisch, V.F., Bott, M., Eikmanns, B.J., 2006. Metabolic engineering of Escherichia coli and Corynebacterium glutamicum for biotechnological production of organic acids and amino acids. Curr. Opin. Microbiol. 9, 268–274.
Wierckx, N.J.P., Ballerstedt, H., de Bont, J.A.M., Wery, J., 2005. Engineering of solvent-tolerant pseudomonas putida S12 for bioproduction of phenol from glucose. Appl. Environ. Microbiol. 71, 8221–8227.
Wietzke, M., Bahl, H., 2012. The redox-sensing protein Rex, a transcriptional regulator of solventogenesis in Clostridium acetobutylicum. Appl. Microbiol. Biotechnol. 96, 749–761.
William Lown, J., 1993. Anthracycline and anthraquinone anticancer agents: Current status and recent developments. Pharmacol. Ther. 60, 185–214.
Woodard, S.I., Dailey, H.A., 1995. Regulation of heme biosynthesis in Escherichia coli. Arch. Biochem. Biophys. 316, 110–115.
Wu, J., Yu, O., Du, G., Zhou, J., Chen, J., 2014. Fine-tuning of the fatty acid pathway by synthetic antisense RNA for enhanced (2S)-naringenin production from L-Tyrosine in Escherichia coli. Appl. Environ. Microbiol. 80, 7283–7292.
Wu, J., Du, G., Chen, J., Zhou, J., 2015. Enhancing flavonoid production by systematically tuning the central metabolic pathways based on a CRISPR interference system in Escherichia coli. Sci. Rep. 5, 13477.
Xiu, Z.-L., Zeng, A.-P., 2008. Present state and perspective of downstream processing of biologically produced 1,3-propanediol and 2,3-butanediol. Appl. Microbiol. Biotechnol. 78, 917–926.
Xu, T., Li, Y., He, Z., Van Nostrand, J.D., Zhou, J., 2017. Cas9 Nickase-Assisted RNA repression enables stable and efficient manipulation of essential metabolic genes in Clostridium cellulolyticum. Front. Microbiol. 8, 1744.
Yakandawala, N., Romeo, T., Friesen, A.D., Madhyastha, S., 2008. Metabolic engineering of Escherichia coli to enhance phenylalanine production. Appl. Microbiol. Biotechnol. 78, 283–291.
Yang, F., Hanna, M.A., Sun, R., 2012. Value-added uses for crude glycerol–a byproduct of biodiesel production. Biotechnol. Biofuels 5, 13.
Yang, J., Camakaris, H., Pittard, J., 2002. Molecular analysis of tyrosine- and phenylalanine-mediated repression of the tyrB promoter by the TyrR protein of Escherichia coli. Mol. Microbiol. 45, 1407–1419.
Yang, P., Liu, W., Cheng, X., Wang, J., Wang, Q., Qi, Q., 2016a. A new strategy for production of 5-aminolevulinic acid in recombinant Corynebacterium glutamicum with high yield. Appl. Environ. Microbiol. 82, 2709–2717.
Yang, S., Fei, Q., Zhang, Y.P., Contreras, L.M., Utturkar, S.M., Brown, S.D., Himmel, M.E., Zhang, M., 2016b. Zymomonas mobilis as a model system for production of biofuels and biochemicals. Microb. Biotechnol. 9, 699–717.
Yang, Y., Lin, Y., Li, L., Linhardt, R.J., Yan, Y., 2015. Regulating malonyl-CoA metabolism via synthetic antisense RNAs for enhanced biosynthesis of natural products. Metab.

Eng. 29, 217–226.
Yazdani, S.S., Gonzalez, R., 2007. Anaerobic fermentation of glycerol: a path to economic viability for the biofuels industry. Curr. Opin. Biotechnol. 18, 213–219.
Yoshinaga, F., Tsuchida, T., Okumura, S., 1974. Method of Producing L-Proline by Fermentation. United States, Patent No. US3819483A.
Zeikus, J.G., Jain, M.K., Elankovan, P., 1999. Biotechnology of succinic acid production and markets for derived industrial products. Appl. Microbiol. Biotechnol. 51, 545–552.
Zhang, A., Schu, D.J., Tjaden, B.C., Storz, G., Gottesman, S., 2013. Mutations in interaction surfaces differentially impact E. coli Hfq association with small RNAs and their mRNA Targets. J. Mol. Biol. 425, 3678–3697.
Zhang, B., Yu, M., Zhou, Y., Ye, B.-C., 2018. Improvement of l-ornithine production by attenuation of argF in engineered Corynebacterium glutamicum S9114. AMB Express 8, 26.
Zhao, Y., Dai, Z., Liang, Y., Yin, M., Ma, K., He, M., Ouyang, H., Teng, C.-B., 2014. Sequence-specific inhibition of microRNA via CRISPR/CRISPRi system. Sci. Rep. 4, 3943.
Zhao, Y., Wang, C.-S., Li, F.-F., Liu, Z.-N., Zhao, G.-R., 2016. Targeted optimization of central carbon metabolism for engineering succinate production in Escherichia coli. BMC Biotechnol. 16, 52.
Zhou, L.-B., Zeng, A.-P., 2015a. Engineering a lysine-ON riboswitch for metabolic control of lysine production in Corynebacterium glutamicum. ACS Synth. Biol. 4, 1335–1340.
Zhou, L.-B., Zeng, A.-P., 2015b. Exploring lysine riboswitch for metabolic flux control and improvement of L-lysine synthesis in Corynebacterium glutamicum. ACS Synth. Biol. 4, 729–734.
Zhou, Q., Shi, Z.-Y., Meng, D.-C., Wu, Q., Chen, J.-C., Chen, G.-Q., 2011. Production of 3-hydroxypropionate homopolymer and poly(3-hydroxypropionate-co-4-hydroxybutyrate) copolymer by recombinant Escherichia coli. Metab. Eng. 13, 777–785.